Linköping Studies in Science and Technology

Dissertation No. 1961

Investigation of nanoparticle-cell interactions for development of next generation of biocompatible MRI contrast agents

Natalia Abrikossova

Division of Molecular Surface Physics and Nanoscience
Department of Physics, Chemistry and Biology
Linköping University, Sweden

Linköping University 2018

Cover: activated neutrophil granulocytes visualized with fluorescence microscopy

Abrikossova, Natalia
Investigation of nanoparticle-cell interactions of next generation of biocompatible MRI contrast agents

ISBN 978-91-7685-190-6
ISSN 0345-7524

Linköping studies in science and technology. Dissertations, No. 1961

Printed in Sweden by LiU-Tryck, Linköping 2018

“There's Plenty of Room at the Bottom”

Richard Phillips Feynman

ABSTRACT

Progress in synthesis technologies and advances in fundamental understanding of materials with low dimensionality has led to the birth of a new scientific field, nanoscience, and to strong expectations of multiple applications of nanomaterials. The physical properties of small particles are unique, bridging the gap between atoms and molecules, on one side, and bulk materials on the other side. The work presented in this thesis investigates the potential of using magnetic nanoparticles as the next generation of contrast agents for biomedical imaging. The focus is on gadolinium-based nanoparticles and cellular activity including the uptake, morphology and production of reactive oxygen species.

Gd ion complexes, like Gd chelates, are used today in the clinic, world-wide. However, there is a need for novel agents, with improved contrast capabilities and increased biocompatibility. One avenue in their design is based on crystalline nanoparticles. It allows to reduce the total number of Gd ions needed for an examination. This can be done by nanotechnology, which allows one to improve and fine tune the physico-chemical properties on the nanomaterial in use, and to increase the number of Gd atoms at a specific site that interact with protons and thereby locally increase the signal. In the present work, synthesis, purification and surface modification of crystalline Gd_2O_3-based nanoparticles have been performed. The nanoparticles are selected on the basis of their physical properties, that is they show enhanced magnetic properties and therefore may be of high potential interest for applications as contrast agents.

The main synthesis method of Gd_2O_3 nanoparticles in this work was the modified "polyol" route, followed by purification of as-synthesized DEG-Gd_2O_3 nanoparticles suspensions. In most cases the purification step involved dialysis of the nanoparticle samples. In this thesis, organosilane were chosen as an exchange agent for further functionalization. Moreover, several paths have been explored for modification of the nanoparticles, including Tb^{3+} doping and capping with sorbitol.

Biocompatibility of the newly designed nanoparticles is a prerequisite for their use in medical applications. Its evaluation is a complex process involving a wide range of biological phenomena. A promising path adopted in this work is to study of nanoparticle interactions with isolated blood cells. In this way one could screen nanomaterial prior to animal studies.

The primary cell type considered in the thesis are polymorphonuclear neutrophils (PMN) which represent a type of the cells of human blood belonging to the granulocyte family of leukocytes. PMNs act as the first defense of the immune system against invading pathogens, which makes them valuable for studies of biocompatibility of newly synthesized nanoparticles. In addition, an immortalized murine alveolar macrophage cell line (MH-S), THP-1 cell line, and Ba/F3 murine bone marrow-derived cell line were considered to investigate the optimization of the cell uptake and to examine the potential of new intracellular contrast agent for magnetic resonance imaging.

In paper I, the nanoparticles were investigated in a cellular system, as potential probes for visualization and targeting intended for bioimaging applications. The production of reactive oxygen species (ROS) by means of luminol-dependent chemiluminescence from human neutrophils was studied in presence of Gd_2O_3 nanoparticles. **In**

paper II, a new design of functionalized ultra-small rare earth-based nanoparticles was reported. The synthesis was done using polyol method followed by PEGylation, and dialysis. Supersmall gadolinium oxide (DEG-Gd2O3) nanoparticles, in the range of 3-5 nm were obtained and carefully characterized. Neutrophil activation after exposure to this nanomaterial was studied by means of fluorescence microscopy. **In paper III,** cell labeling with Gd_2O_3 nanoparticles in hematopoietic cells was monitored by magnetic resonance imaging (MRI). **In paper IV,** ultra-small gadolinium oxide nanoparticles doped with terbium ions were synthesized as a potentially bifunctional material with both fluorescent and magnetic contrast agent properties. Paramagnetic behavior was studied. MRI contrast enhancement was received, and the luminescent/fluorescent property of the particles was attributable to the Tb3+ ion located on the crystal lattice of the Gd_2O_3 host. Fluorescent labeling of living cells was obtained. **In manuscript V,** neutrophil granulocytes were investigated with rapid cell signaling communicative processes in time frame of minutes, and their response to cerium-oxide based nanoparticles were monitored using capacitive sensors based on Lab-on-a-chip technology. This showed the potential of label free method used to measure oxidative stress of neutrophil granulocytes. In **manuscript VI,** investigations of cell-(DEG-Gd_2O_3) nanoparticle interactions were carried out. Plain (DEG-Gd_2O_3) nanoparticles, (DEG-Gd_2O_3) nanoparticles in presence of sorbitol and (DEG-Gd_2O_3) nanoparticles capped with sorbitol were studied. Relaxation studies and measurements of the reactive oxygen species production by neutrophils were based on chemiluminescence. Cell morphology was evaluated as a parameter of the nanoparticle induced inflammatory response by means of the fluorescence microscopy.

The thesis demonstrates high potential of novel Gd_2O_3-based nanoparticles for development of the next generation contrast agents, that is to find biocompatible compounds with high relaxivity that can be detected at lower doses, and in the future enable targeting to provide great local contrast.

Populärvetenskaplig sammanfattning

De små nanopartiklarnas fysikaliska egenskaper är unika, och befinner sig i gränslandet mellan atomer och molekyler, å ena sidan och bulkmaterial å andra sidan. Arbetet som presenteras i denna avhandling visar på möjligheten att använda flera olika typer av nanopartiklar för biomedicinsk bildbehandling, med särskild inriktning på kontrastmedel för signalförstärkning vid magnetisk resonansbildning (MRI). Syntes, upprening, ytmodifiering och karakterisering av både kristallina Gd2O3-nanopartiklar har gjorts. Dessa nanopartiklar har valts utifrån deras fysikaliska och kemiska egenskaper, det vill säga de uppvisar förbättrade magnetiska egenskaper och kan därför vara högintressanta för tillämpningar såsom kontrastmedel inom biomedicinsk avbildning. En stor utmaning vid utformning av nya kontrastmedel baserade på nanopartiklar (jämfört med Gd-komplex som idag används inom sjukvården på klinik världen över) är att minska det totala antalet Gd som behövs för en undersökning. Detta kan göras genom nanoteknik, dvs att förbättra och finjustera de fysikalisk-kemiska egenskaperna hos det nanomaterial som används. Vidare öppnar sig möjligheter för målsökande nanoprober, då kan man ytterligare öka signalen, genom att endast lokalt öka koncentrationen av Gd-joner på en specifik plats eller sätt leder detta till en förstärkt signal. En nanopartikel består av ca 1000 Gd joner vilket möjliggör en 1000-falt förstärkt kontrast lokalt jämfört med de existerande kontrastmedlen som endast bär en Gd-jon per komplex. Det är också av högsta relevans att utvärdera effekter av nanopartiklar i biologiska system. Cellstudier har potential att ersätta och / eller minska användandet av djurförsök. Detta är i linje med nya strategier för riskbedömning av kemikalier där man vill ersätta/reducera antalet djurförsök med mer prediktiva test. Syftet med denna avhandling är att undersöka biokompatibiliteten hos lovande nanopartiklar som syntetiserats av mig och andra medlemmar av vårt forskarteam. Långsiktigt vill man åstadkomma effektivare, billigare och mer relevant riskbedömning av kemikalier och kombinationer av kemikalier. Detta kommer att kunna uppnås genom ökad kunskap om effekterna på människor och med hjälp av nya celltester. Dessa studier kräver nära samarbete mellan olika vetenskapliga discipliner, dvs medicin, biologi, kemi och fysik. En slående fördel med detta tillvägagångssätt är att resultatet av flera strategier gällande nanopartikel-funktionalisering kan utvärderas med hjälp av fysisk karaktärisering, probing-kapacitet och biologisk aktivitet redan i ett tidigt skede, under design och optimering av en ny typ av nanopartikel, vilket stämmer väl överens med den internationella rekommendationen ”safe by design” för framtidens hållbara nanomaterial. Biokompatibiliteten förbättras med hjälp av olika tekniker, t.ex. olika syntesvägar, via capping, ytmodifiering och funktionalisering, samt genom att introducera en liten mängd av något annat element/grundämne. För att studera cell-nanopartikel interaktion används isolerade blodceller såsom neutrofila granulocyter, men även cell-linjer THP-1 och makrofager från mus-lungvävnad. Våra in vitro-studier inkluderar undersökning av effekterna av Gd_2O_3 nanopartiklar på funktionen av neutrofila granulocyter med avseende på produktion av reaktiva syremetaboliter.

List of publications

Paper I

Natalia Abrikossova, Caroline Skoglund, Maria Ahren, Torbjörn Bengtsson and Kajsa Uvdal
Effects of gadolinium oxide nanoparticles on the oxidative burst from human neutrophil granulocytes.
Nanotechnology 2012;23(27); 275101.

Paper II

Maria Ahren, Linnea Selegård, Anna Klasson, Fredrik Söderlind, Natalia Abrikossova, Caroline Skoglund, Torbjörn Bengtsson, Maria Engström, Per-Olov Käll and Kajsa Uvdal
Synthesis and Characterization of PEGylated Gd_2O_3 Nanoparticles for MRI Contrast Enhancement.
Langmuir 2010;26(8):5753-62.

Paper III

Anna Hedlund, Maria Ahrén, Håkan Gustafsson, Natalia Abrikossova, Marcel Warntjes, Jan-Ingvar Jönsson, Kajsa Uvdal, Maria Engström.
Gd_2O_3 nanoparticles in hematopoietic cells for MRI contrast enhancement.
International Journal of Nanomedicine. 2011;6:3233-40.

Paper IV

Rodrigo M. Petoral, Jr., Fredrik Söderlind, Anna Klasson, Anke Suska, Marc A. Fortin, Natalia Abrikossova, Linnea Selegård, Per-Olov Käll, Maria Engström and Kajsa Uvdal
Synthesis and Characterization of Tb^{3+}-Doped Gd_2O_3 Nanocrystals: A Bifunctional Material with Combined Fluorescent Labeling and MRI Contrast Agent Properties.
Journal of Physical Chemistry C. 2009;113(17):6913-20.

Paper V

Kalle Bunnfors, Natalia Abrikossova, Joni Kilpijärvi, Peter Eriksson, Jari Juuti, Niina Halonen, Caroline Brommesson Anita Lloyd Spets and Kajsa Uvdal

Lab-on-a chip for capacitive measurements on human neutrophil granulocytes and their activation triggered by Ce/Gd oxide nanoparticles. In manuscript

Paper VI

Natalia Abrikossova, Caroline Brommesson, Emanuel Larsson, Peter Eriksson, Zhangjun Hu and Kajsa Uvdal

Sorbitol capping of gadolinium oxide nanoparticles for magnetic resonance imaging contrast enhancement. In manuscript

Related papers not included in thesis:

Emanuel Larsson, Christian Dullin, Natalia Abrikossova, Caroline Brommesson, Urša Mikas, Chiara Garrovo, Agostino Accardo, GiulianaTromba, Igor Serša, Kajsa Uvdal.

Optimization of the loading efficacy for dual-modal CT/MRI macrophage tracking in lungs of an asthma mouse model. Manuscript.

Emanuel Larsson, Christian Dullin, Natalia Abrikossova, Urša Mikas, Caroline Brommesson, Chiara Garrovo, Agostino Accardo, GiulianaTromba, Kajsa Uvdal, Igor Serša.

Dual-modal CT and MRI functional and anatomical imaging using barium sulphate and gadolinium nanoparticle loaded macrophages in a preclinical asthma mouse mode. Manuscript.

Linnea Selegård, Alexei Zakharov, Andreas Skallberg, Natalia Abrikossova, Kajsa Uvdal.

PEEM, LEED and PES temperature study of Eu doped Gd_2O_3 nanoparticles and their interactions with silicon. Manuscript.

Author contributions

Paper I

I was responsible for the study design and implementation, including synthesis of nanoparticles, isolation of neutrophils, measurements of ROS, and examination of the cellular behavior and morphological changes by fluorescence staining. I was responsible for summarizing the results and writing the major part of the manuscript.

Paper II

I carried out synthesis of gadolinium oxide (DEG- Gd_2O_3) nanoparticles followed by their PEGylation, and dialysis. I was responsible for studies of neutrophil activation after exposure to this nanomaterial by means of fluorescence microscopy and contributed to the manuscript writing.

Paper III

I carried out synthesis of gadolinium oxide (DEG- Gd_2O_3) nanoparticles. I participated in culturing and labeling of a monocytic cell line, THP-1, MRI measurements and contributed to the manuscript writing.

Paper IV

I acquired a knowledge on synthesis of gadolinium oxide nanoparticles doped with rare-earth ions. I was involved in sample preparation for the microscopy analysis of THP-1 cell line incubated with the particles and contributed to the manuscript writing.

Paper V

I participated in the project planning and design of the study. I carried out isolation of neutrophils and initiated testing of the Lab-on-a-chip principle based on the CMOS/LTCC sensor device to monitor the neutrophils activity. I participated in analysis of the results and contributed to the manuscript writing.

Paper VI

I was responsible for the study design and implementation. I carried out gadolinium oxide nanoparticles synthesis and their surface modification, relaxivity measurements

using Bruker minispec mq60 NMR analyzer, macrophage cell line culturing and labeling, isolation of human neutrophil granulocytes, measurements of ROS, and examination of the cellular behavior and morphological changes by fluorescence staining. I was responsible for summarizing the results and writing the major part of the manuscript.

Acknowledgement

First of all, I would like to thank to my principal supervisor, Kajsa Uvdal, for giving me a chance to do research, for sharing your knowledge with me, for your patience and valuable discussion. You opened to me an exciting field of nanomaterials. Your visionary advice to focus on studies of cellular activity determined the main direction of my work. Your energy and optimism helped me all the way, from my first experiment to summarizing the results in this thesis. Your leadership was stimulating. Fantastic atmosphere of friendship, collaboration and engagement in your group is something that I would nether forget. Last, but not least, I truly appreciate your understanding of my wish to work part time to combine my research and my family in a way that suited me best.

I am deeply grateful to my co-supervisor, Caroline Brommesson for continuous and friendly support. Carro, you are great teacher! You thought me to deal with cells, to make advanced measurements on uptake, morphology and production of reactive oxygen species, to collect and analyze results. We spent many hours together, and working with you was a real pleasure.

I would like to thank Maria Engström for introducing me into field of MRI science and biomedical imaging.

Maria Sunnerhagen was my mentor during all these years. Thank you, Maria for keeping me focused!

I would like to express my sincere gratitude to all persons around me who supported me in different ways. Many thanks to all the current members and alumni of Molecular Surface Physics and Nanoscience Division: Maria, Linnea S, Cecilia, Linnea A, Andreas, Peter, Kalle, Zhangjun, Xuanjun, Frank and Jiwen for interesting discussions and nice time together.

I would like to acknowledge all my co-authors: Torbjörn Bengtsson, Maria Ahren, Linnea Selegård, Anna Hedlund, Emanuel Larsson, Peter Eriksson, Zhangjun Hu, Per-Olov Käll, Fredrik Söderlund, Håkan Gustafsson, Anita Lloyd Spets, Joni Kilpijärvi, Anke Suska. Interactions with you were extremely useful for my thesis work.

All my friends, colleagues and collaborates at IFM, thank you for your assistance and for building the department where excellent science is combined with continuous consideration and improvement of work environment.

Finally, I would like to take the opportunity to thank my family and my friends for encouragement and support.

Tack alla!

Linköping, November 2018

Natalia Abrikossova

Abbreviations

DEG	Diethylene glycol
DIC	Differential interference contrast
DLS	Dynamic light scattering
DTPA	Diethyltriamine pentaacetic acid
fMPL	N-formyl-methionyl-leucyl-phenylalanine
IR	Infrared spectroscopy
MRI	Magnetic resonance imaging
MPTES	3-mercaptopropyl trimethoxy silane
NADPH	Nicotinamide adenine dinucleotide phosphate
NEXAFS	Near-edge X-ray absorption fine structure spectroscopy
NMR	Nuclear magnetic resonance
PBS	Phosphate buffered saline
PEG	Polyethylene glycol
PMA	Phorbol 12-myristate 13-acetate
PMN	Polymorphonuclear granulocytes
RES	Reticuloendothelial system
RF	Radio frequency
ROS	Reactive oxygen species
TEM	Transmission electron microscopy
XPD	X-ray diffraction
XPS	X-ray photoelectron spectroscopy

Table of Contents

Chapter 1

Nanoparticles: general definitions

1.1. Nanomaterials in modern science in technology

Most formal definitions of engineered nanomaterials revolve around the manipulation of materials roughly 1 to 100 nm in size[1]. Recent progress in synthesis technologies, as well as advances in fundamental understanding of materials with low dimensionalities, coupled to strong expectation in terms of applications boosted huge interest in the field, and led to the birth of a new scientific discipline, the nanoscience. It is important to underline, that the size is not the sole reason for the interest, and it cannot be used as the only motivation for studies and use of nanomaterials. The point is that physical properties of small particles are unique, bridging the gap between atoms and molecules, on one side, and bulk materials on the other side.

In particular, the main distinction of a nanomaterial from its bulk counterpart is considered to be the presence of quantum effects in the former. Indeed, at the atomic scale, electronic states are typically characterized by discrete energy levels that are often separated by electron volts; the spatial distribution of these states is highly localized. In contrast, electronic states in crystalline matter are typically characterized by energy bands: the energy states form a quasicontinuous spectrum with delocalized spatial distributions. A nano-particles in this scheme may possess hundreds or thousands of atoms. Therefore, at the nanoscale the distribution of energy states resides between these limits: there are many states within energy interval of the order of 1 eV, but the states are still separated from each other[2].

This evolution of an energy level from an atom towards bulk systems through the nano-particle is illustrated in Figure 1.1. The confinement effects in a nanomaterial make quantum effects stronger in comparison to the bulk materials, leading to qualitatively new physical properties of the former. Moreover, the electronic, optical and magnetic properties of small particles, has a non-linear behavior between the two general limits given by the atomic and the bulk-like behavior[3-4]. In particular, small clusters show substantial dependence of magnetic properties, e.g. orbital and spin moments, as well as interactions between magnetic moments in the system on its dimensionality and size. Improved fundamental

knowledge of the behavior of nanomaterials is of crucial importance for their applications.

The small size of the nanoparticles is essential for their practical use. Indeed, a 10 nm particle (Figure 1.2) is too tiny for us to observe with a naked eye, and consequently, to operate nanoparticles in a standard way, as we deal with bulk materials and conventional engineering tools. Nanoparticles, for instance, can be suspended in fluids, the so-called nanofluids[5]. Due to the small size of the nanoparticles, their Brownian motion caused by collision with surrounding fluid molecules is sufficient to overcome gravitational force. Properly chosen nanoparticles will enhance the thermal, electrical, magnetic, and/or chemical properties of the original fluid. Moreover, if they are designed in a way that prevents their agglomeration, they will remain suspended and can be used in applications, which are discussed in this thesis. Another possibility to use the nanoparticles is to collect them on an appropriate substrate.

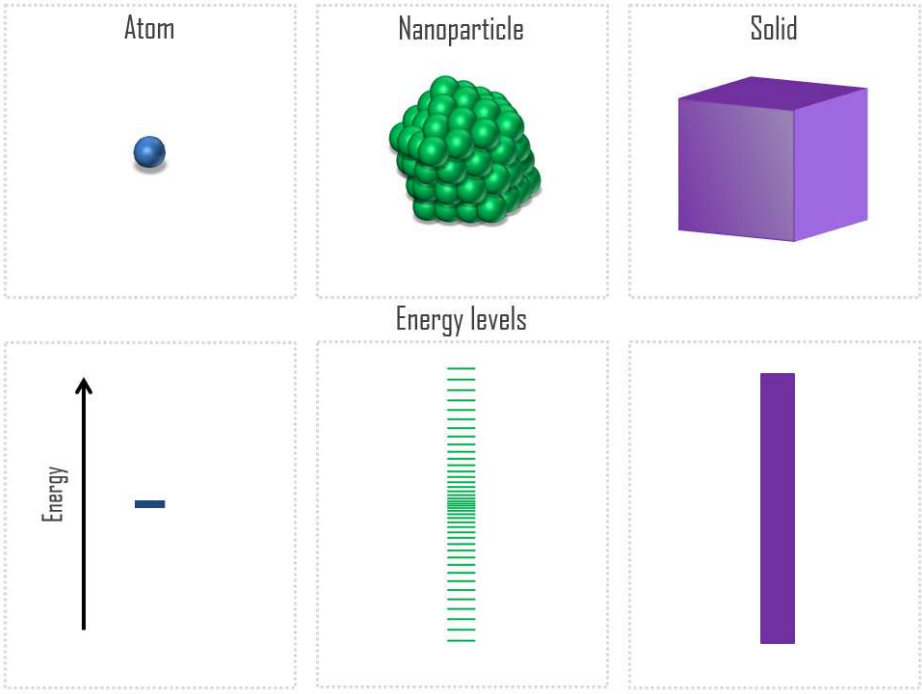

Figure 1.1 Evolution of electronic states from atom via nanoparticle towards bulk solid.

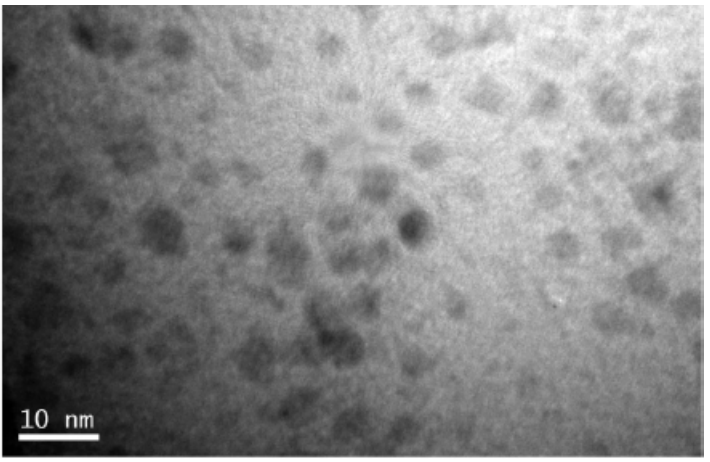

Figure 1.2 Transmission electron microscope (TEM) image of as-synthesized DEG-capped 5Tb:Gd (5Tb:Gd-DEG) nanoparticle. Reprinted with permission from Paper IV. Copyright 2009 American Chemical Society.

Quantum phenomena are enhanced in the nanoparticles due to their small size (Figure 1.1) and determine majority of their applications in modern science in technology, existing, as well as potential. Let us consider, for example, a metallic nanoparticle interacting with a quantum of light, with a photon. The oscillating electromagnetic field leads to a collective motion of the nanoparticles valence electrons, or to the so-called plasmon oscillations. The plasmons may be localized at the surface of the nanoparticles, in which case they are called surface plasmons. The plasmonic response becomes heightened at a resonance optical frequency that depends on the size and shape of the nanoparticles, as well as on the density of its valence, mostly free-like, electrons[5]. Varying these parameters, one can ensure that plasmons resonate in specific, well-defined bands ranging from ultraviolet to infrared parts of the spectrum, depending on the need for a specific application. Interestingly, this is perhaps the first known application of the nanoparticles, dating back to ancient Rome technology of making glass with varying color. Nowadays, nanofluids which exploit a physical phenomenon of plasmon resonance have been deployed in biological imaging and tumor-destroying hypothermia treatments, and they constantly find new appli-

cations, e.g. in photovoltaic thermal collectors that generate electricity and usable heat simultaneously[5].

A strong motivation to study nanoparticles is their use in heterogeneous catalysis. A catalyst increases the rate of a chemical reaction, and therefore it is very important and often used in the chemical and pharmaceutical industries[6]. The catalytic activity depends critically on the number of active sites, which makes nanoparticles superior in the applications. Catalysts are often designed by dispersion of sub-nanometer and nano-sized metal particles on oxide supports[7].

A rapidly growing field for applications of nano-systems is their use for sensing. Their functionality is related to the quantum confinement effect. For example, the size-dependent band gap of a nanomaterial may result in a variable photoluminescence emission. The adsorption of certain ions or molecules could modify the gap, quenching or enhancing photoluminescence. Optical detection of the change can be utilized for sensing of the ions or molecules[8]. In fact, biosafety regulations requiring rapid and cost-effective evaluations give strong motivation for development of novel sensors, often involving nano-systems. For example, traditional methods for *in vitro* cytotoxicity evaluation are often expensive and time-consuming, because they include cell cultivation and label-based assay kits. This has led to a growing interest in noninvasive, label-free, real-time, data-rich biosensing techniques, like surface plasmon resonance spectroscopy, electrochemical quartz crystal microbalance measurements, optical sensing, impedimetric sensing, and capacitive sensing[9]. In particular, cell-impedance measurement using the lab-on-a-chip (LoC) concept has been used in this work, Paper V. Moreover, nanoprobes combining different modalities, for instance magnetic resonance imaging and fluorescence attract increasing interest, e.g. as a useful tool for biomedical imaging[10].

Magnetism is another quantum phenomenon, which is important for applications of nanoparticles in general, and in particular for imaging applications in medicine[11]. The source of magnetism in condensed matter is identified with the spin of the electrons. The spontaneous ordering of the magnetic moments on individual atoms in a material, known as ferromagnetism (FM) or antiferromagnetism (AFM). It is a manifestation of electrostatic Coulomb interactions constrained by Pauli's exclusion principle, which forbid the occupancy of a quantum state by two electrons with the same spin[12]. Note that in contrast to the free-electron behavior important for plasmonic nanoparticles, the electrons that most

often contribute to magnetic phenomena are localized electrons belonging to *d* or *f* shells of the atoms. With temperature increasing above specific limit, known as Curie temperature T_C of a ferromagnet or as a Neel temperature T_N of an antiferromagnet, the net magnetization of the material vanishes, and the material becomes paramagnetic (PM). Note, however, that the local magnetic moments still exist in most magnetic materials in their PM phase above T_C or T_N, and net magnetization vanishes due to the disorder of the local moments.

Even below T_C or T_N bulk FM (AFM) materials may be demagnetized on the macroscopic scale in the absence of magnetic field because the existence of magnetic domains: microscopic, but still large enough parts of the material with FM(AFM) order inside each domain, but with disordered orientation of magnetization between the domains due to magnetic dipolar interactions. However, magnetic behavior can be influenced by scaling down the system size[11,13]. In particular, magnetic nanoparticles can be made small enough to remain in the monodomain magnetic state, which gives qualitatively new opportunities for their applications. For example, consider FM nanoparticles in the monodomain state. Their individual magnetization directions will be disoriented with respect to each other in the absence of magnetic field, and the temperature will flip the directions randomly, making them similar to the bulk PM material. However, their magnetization directions will order in the magnetic field. Because their moments, which are proportional to number of atoms in the nanoparticles, are larger than moments of individual atoms, the magnetic susceptibility of the nanoparticles will be much larger as well. This gives rise to the phenomenon of superparamagnetism. In fact, interest in magnetic nanoparticles has increased in the past few years because of the high potential of their applications in several fields, like ultrahigh-density recording and medicine. The latter is of primary interest for this work.

1.2. Nanoparticles properties enabling biomedical application

In the past year one of the most promising and rapidly developing areas of the use of magnetic nanoparticles is their applications in biomedicine. When the size of a particle decreases from the micro- to nano-meters, their magnetic state is often strongly affected. In particular, the reduction of the size makes the particles effectively one-dimensional, leading to the appearance of the superparamagnetic effects [14-15]. In this respect,

metal oxide nanoparticles attract substantial attention, because of their general availability, well-developed synthesis methodologies, relatively straight-forward manipulation to obtain controlled magnetic behavior and acceptable levels of magnetic signal. The possibility to control their behavior with an external the magnetic field makes magnetic nanoparticles into highly attractive material. Indeed, they possess appropriate physicochemistry and their surface properties may be tailored via surface modification, Superparamagnetic nanoparticles of iron oxide, have earlier been shown to produce negative contrast in Magnetic Resonance Imaging (MRI). The Uvdal group at Linköping University has shown that when scaling down in size this material, with a size of 2-6 nm, capped with a passivizing non-ionic material, is very promising as positive contrast agent[11,13]. This shows the potential in nanomaterial design for biomedical imaging.

The magnetic nanoparticles have been extensively investigated for various applications, such as drug delivery, tissue engineering and repair, biosensing, biochemical separations, and bioanalysis. In the field of disease therapy, the development of "theragnostics", which facilitates simultaneous drug delivery and imaging, represents an important breakthrough[16].

In addition, ferromagnetic magnetite nanoparticles are characterized by very high values of magnetization and coercive force, which ignites a considerable interest, for example, for their use for therapeutic purposes[17]. For instance, an application of ferrofluids for the treatment of oncological diseases by local hyperthermia was proposed in the beginning of 1990s. Jordan et al.[18] has proved high efficiency of the conversion of the energy absorbed by suspension of superparamagnetic nanoparticles in an oscillating magnetic field into heat. The effect can be used *in vivo* to destroy the pathological cells by heating certain tumor tissues, the so-called "leaky cells". Preclinical and clinical data show that hyperthermia is in fact feasible and effective in combination with radiation therapy[19].

Of course, lot of research must still be undertaken to address multiple challenges faced in nanomedicine and to ensure safe and efficient biomedical applications of magnetic nanoparticles. Considering metal toxicity and pharmacology important issues must be addressed, such as dose response, kinetics etc. Indeed, the biochemical and physiological effects of the nanoparticles depend upon the chemical form of the metal, e.g. oxidation state, salt or complex. Moreover, toxicity is dependent upon the route of exposure[20]. Accurate analytical tools need to be de-

veloped further for studies of interactions of nanoparticles with the immune system. A wise strategy is to screen nanoparticle on the cellular level, in parallel with nanomaterial design, synthesis and development. This is also the strategy we used in Paper I, where Gd_2O_3 nanoparticles of our own design were tested in presence of blood cells, more specifically, neutrophils. The cellular response on the presence of three sets of Gd_2O_3 nanoparticles was investigated, i.e. as synthesized, dialyzed and functionalized and dialyzed, and an increase of their biocompatibility by the surface modification of these nanoparticles with polyethylene glycol (PEG) was demonstrated. In such a way one obtains an early sign on the nanomaterial with high potential, as well as at early stage sort out material with negative response. This is also in line with the strive, nationally and internationally (EU, USA) that present and future material development should involve sustainability from step one, in this case, **safe by design.**

Finally, multiple preclinical and clinical studies in relevant animal models and disease states will be required to substantiate proof of concept using different controls especially in MRI molecular imaging. Safety and biocompatibility studies, in particular long-term toxicity studies, will be required, as well in addition to proof-of-concept studies[19]. Thus, the development of methodologies for efficient evaluation and improvement of biomedical performance of novel nanoparticles at the initial stages of their design is of primary importance. This is the subject of the present thesis.

Chapter 2

Synthesis of nanoparticles

2.1. General overview of synthesis methods.

Rapid development of techniques for synthesis of nanoclusters has resulted in remarkable advances in our knowledge of these systems and pathed the way to their advanced applications in different fields, from physics and chemistry to biology and medicine. Already in the 1960s cluster sources were developed to produce metallic clusters[21]. However, they were composed of only a few atoms in the gas phase. In the first half of the 1980s clusters of alkali metals with up to about 100 atoms were produced and detected[22]. This has modified the perception of these systems originally viewed as a kind of small molecules and stimulated the development of numerous synthesis techniques. For instance, seeded supersonic nozzle sources are used to produce intense cluster beams of low-boiling-point metals. Gas-aggregation sources are particularly efficient in the production of large clusters with more than 10000 atoms of low-to-medium-boiling-point materials. Laser vaporization sources produce clusters in the size range from the atom to typically several hundreds of atoms per cluster. In pulsed-arc cluster-ion sources an intense electrical discharge rather than a laser is used to produce the clusters. Ion sputtering sources are primarily used to produce intense continuous beams of small singly ionized clusters of most metals. Liquid-metal ion sources produce singly and multiply ionized clusters of low-melting-point metals[23].

2.2. Wet chemistry synthesis

Efficient methods for nanoparticle synthesis employ chemical reactions in the so-called “wet-chemistry” synthesis[16]. For example, in the sol−gel method the hydroxylation and condensation of precursors in a solution phase yields a colloidal solution (sol) of nanosized particles. Oxidation method can, for instance, be used for the synthesis of small-sized ferrite colloids, like Fe_3O_4 by crystallization starting from the ferrous hydroxide gels. It involves partial oxidation of the Fe(II) hydroxide suspensions with different agents (e.g., nitrate ions). The hydrothermal synthesis method is used to synthesize nanoparticles in aqueous media in reac-

tors or autoclaves at high temperature, above 200 °C and high pressure. This allows one to achieve the formation of small-sized NPs due to rapid nucleation and faster growth.

Further discussion of numerous of "wet-chemistry" synthesis techniques can be found in Ref.[16], where the authors also point out considerable efforts that have been spent in the development of magnetic nanoparticles (MNPs), because of their applicability in many different areas, for example for bioimaging[10,15]. Precise control over the synthesis conditions and surface functionalization of MNPs is pointed out as the central issue. Indeed, it governs the physical, as well as chemical properties of the nanoparticles, their stability, and their biocompatibility. The following conditions are of primary importance for pharmaceutical and biomedical purposes:

- the nanoparticles should possess very small size and narrow size distribution;
- magnetization values must be high;
- high magnetic susceptibility for an optimum magnetic enrichment must be combined with loss of magnetization after removal of the magnetic field;
- optimal surface coating must ensure tolerance and biocompatibility, as well as specific localization at the biological target site.

Concluding this section, it is worth to note that the synthesis of nanoparticles, especially those that exhibit superparamagnetic properties of interest for this thesis, is a complex process because of their colloidal nature[19]. There are several reasons for this. Most importantly, there is a need to defining experimental conditions, leading to a monodisperse population of magnetic grains of suitable size. Next, the process must be reproducible, and in addition it should be possible to industrialize it in such a way that complex purification procedures (like ultracentrifugation, size-exclusion chromatography, magnetic filtration, or flow field gradient) are not needed. Thus, it is challenging to use wet-chemistry-based process for the synthesis of sophisticated nanomaterials with homogeneous composition and narrow size distribution. At the same time, in order to design nanoprobes with unique capabilities to deliver enhanced local signal contrast in MRI very high control of the nanoprobe shape and geometry becomes very important for selective cell uptake. Moreover, the requirements for the future nanoprobes will increase regarding both hard core (core/shell) and soft outer bio-shell. Therefore, novel synthesis techniques could be of interest for future research[24].

2.3. Modified "polyol" synthesis method

Precipitation in a high boiling alcohol (polyol method) has been used with success for the synthesis of sub-micrometer transition metal particles and selected oxides. In 2003 Bazzi *et al.*[25] employed this route to prepare colloidal suspension of lanthanide nano-oxides with the aim to incorporate lanthanide impurities in ultra-small, sub-5-nm metal oxide hosts. The technique is now known as modified "polyol" protocol. Studying the direct precipitation of rare earth doped oxides from metallic salts in polyalcohol, Bazzi *et al.* mixed suitable rare earth precursors, $LnCl3 \cdot 6H_20$ with Ln=Eu, Tb, Nd, Gd or Y with a defined amount of water in a high boiling diethylene glycol (DEG). To reduce the possibility of lanthanide hydroxide formation, the precipitation was carried out in a non-aqueous environment. Indeed, Bazzi *et al.* observed the formation of oxide, rather than hydroxide particles, and explained this by the dehydrating properties of the alcohol associated with the high temperature of the solution during the synthesis.

One year later, Bazzi *et al.* further refined the modified "polyol" protocol and made it highly suitable for the synthesis of the magnetic nanoparticles. In this work, we primarily use this protocol, so we describe it in details below following closely the original description of Bazzi *et al.*[26].

All reactions should occur at temperatures lower than 200°C. Rare-earth chloride $RECl_3 \cdot 6H_2O$ with RE = Eu, Gd, or Y (99.9% Aldrich) should be dispersed in 20 ml of DEG with a global metal concentration of 0.1–0.5 mol l^{-1}. After strong stirring for 30 min, 1 ml of aqueous NaOH solution (3mol/l) should be added and the mixture should be heated in a silicon oil bath at 140°C for 1 h. After complete dissolution of the compounds, the solution should be heated at 180°C for 4 h under vigorous stirring in refluxing DEG.

In the experiment of Bazzi *et al.*, the procedure described above resulted in transparent suspensions of particles dispersed in organic solvent. Monitoring the oxide particle suspension, the authors concluded that it was colloidally stable for weeks, independently of the particles content (pure Eu, Eu/Gd or Eu/Y solid solution oxides). Moreover, the nanoparticles consisted of a single phase. At the same time, the initial metal ion concentration influenced the size of the synthesized particles. Bazzi *et al.* suggested that varying the concentration one could adjust the size to some degree, though the main parameter for controlling the

grain size in their experiment was water/DEG ratio, because it was found to directly determine the nucleation rate. The duration of heating at 180°C was also important, and it was set to 4 h in the experiment, because longer treatment did not lead to further increase of the grain size.

Bazzi *et al.* recommended to ensure that OH^- concentration of the starting solution should be small. This prevented the rapid precipitation of hydroxides in his experiment. The addition of one equivalent of NaOH was thus suggested to be a good compromise. Lower values were found to give too small reaction yields while higher values led to irreversible precipitation of hydroxides.

An important suggestion by Bazzi *et al.* was to dialyze the obtained colloidal suspension against pure DEG for 24 h to achieve purification. In addition, the authors verified that a partial low-pressure distillation of solvent could be performed to achieve concentrated suspension. In summary, the protocol described above allowed the authors of Ref.[26] to obtain solution containing up to 10 wt% rare earth oxide without particle agglomeration.

As motioned above, DEG process the main contribution to stabilize the nanoparticles in DEG solution. Other capping molecules also can be added during the synthesis. For instance, Söderlind and coworkers studied that the addition of oleic acids can give oleic acid-stabilized Gd_2O_3 nanoparticles, which can be well-dispersed in non-polar solvents. However, it is not suitable for MRI applications due to its poor water-solubility[27].

Meanwhile, our group has made efforts to apply the nanoparticle synthesized from this method for biological studies. We used Bazzi's method to obtain the DEG-suspended Gd_2O_3 nanoparticles, but the dialysis of the as-synthesized Gd_2O_3 nanoparticles was processed against milli-Q water instead of DEG. In Paper I, we showed that the presence of DEG, even in a low amount, can induce negative effects on neutrophil granulocytes. Actually, the small amount of DEG on the surface of Gd_2O_3 after dialysis could be easily exchanged by customized PEGylated-molecules. Paper II demonstrated that the delivered pegylated Gd_2O_3 exhibits much better biocompatibility and is very promising for MRI application.

Chapter 3

Methods of nanoparticles characterization

The properties of nanoparticles and their performance in applications depend crucially on the chemical composition, the size and the shape of the particles, as well as on their microstructure. In addition, for biomedical applications the polydispersity, charge, and nature of the coating play essential role[19]. Because of the small size of the nanoparticles, most advanced experimental techniques must be employed for the characterization of the above-mentioned properties.

In fact, it is not straightforward to define unambiguously what is the size of the nanoparticle. Is the size determined by the crystalline part alone? How should we characterize the size for nanoparticles consisting of the core, the shell, and the cover layers? Moreover, even state-of-the-art synthesis protocols most often give polydisperse nanoparticles with certain heterogeneity of sizes. In order to study the size distribution, the shape and crystallinity of the particles transmission electron microscopy (TEM) is often employed[15,28-30]. Moreover, high-resolution transmission electron microscopy (HRTEM) allows one to investigate the structure with atomic-scale resolution, as well as to get access to local microstructures and defects, like lattice vacancies, as well as to characterize structural and chemical parameters of particles surfaces[31].

X-ray diffraction (XRD) experiments can be performed to determine the crystalline structure of the particles. In addition, intensity of a diffraction pattern can be used to quantify the proportion of different phases formed in a mixture[15,32]. Extended X-ray absorption fine structure (EXAFS) also gives information on the particle size. Moreover, it has recently been demonstrated that near edge X-ray absorption fine structure (NEXAFS) studies can be used to characterize oxidation states of chemical elements composing nanoparticles[30]. The advantage of the energy dispersive X-ray diffraction (EDXD) is that it can be carried out on the suspension leading to an improved knowledge of fine structural details.

Photon correlation spectroscopy (PCS), also called dynamic light scattering (DLS) or quasi-elastic light scattering (QELS), gives access to the so-called hydrodynamic radius of a particle and to the polydispersity of the colloidal solution[33]. In addition, the DLS can be utilized to

study the stability of the nanoparticles. X-ray photoelectron spectroscopy (XPS) and infrared spectroscopy (IR) are powerful experimental techniques for molecular composition analysis[15,29-30].

To investigate the surface properties of coated nanoparticles, to characterize the bonding between the particle surface and the coating as well as to understand the influence of the coating on the magnetic properties of the nanoparticles, several experimental techniques can be used, including atomic and chemical force microscopy (AFM and CFM), Fourier transform infrared spectroscopy (FTIR), as well as other techniques reviewed in Ref. [19]. Below we present more detailed description of the experimental techniques, which are most relevant for this thesis.

3.1. Transmission Electron Microscopy

XRD experiments that are traditionally used for highly precise structural characterization of solids, give access to the average structure of the studied materials. However, they are not suitable for studies of local regions of a specific material, and its applicability for studies of individual nanostructures is limited. At the same time, there is an interest and a great need in a detailed characterization of nanomaterials with atomic-scale resolution. This makes the transmission electron microscopy highly attractive for applications in the field. Indeed, it is capable to form images of atomic arrangements at localized regions within materials[34]. In the TEM one uses electrons for imaging of the studied materials. In contrast to X-rays, the electrons are negatively charged, and therefore it is possible to accelerate them using the electron guns, as well as to focus them using the electromagnetic fields of advanced systems of lenses (see Figure 3.1). Moreover, the electrons scattered by samples can be further collected by lenses to form true images in real space, in the sense that each point of the image in principle corresponds to a specific point of the sample. In this respect, TEM is similar to optical microscopes.

Importantly, for accelerating voltage of 1000 kV, the electron wavelengths are of the order of 0.001 nm[34], which should be more than sufficient for the resolution with the atomic scale. Moreover, a combination of TEM with electron energy loss spectroscopy (EELS) allows one for a chemical analysis of the samples at the atomic scale.

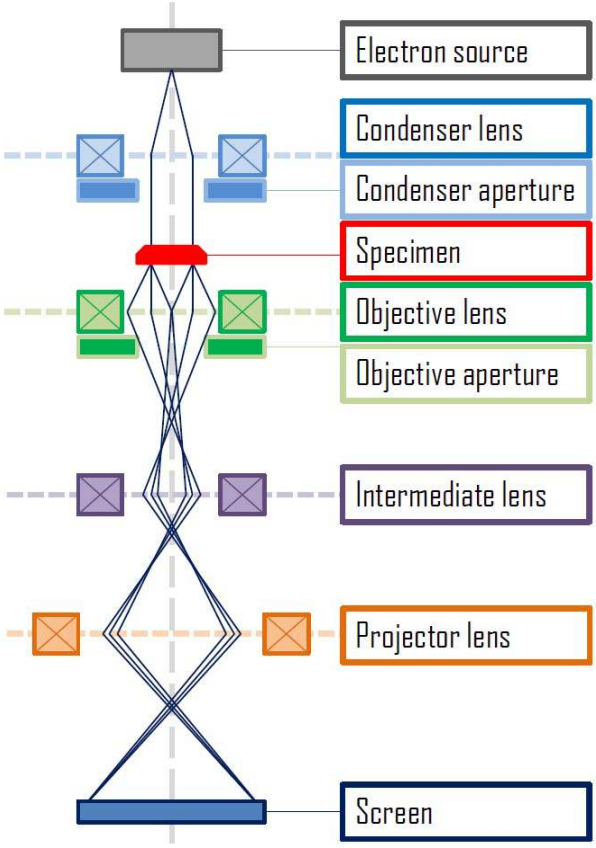

Figure 3.1 Basic set up for transmission electron microscopy in the imaging mode

In reality, there are limitations. Perhaps the most essential here are the so-called aberrations because the lenses are not perfect, and they create magnetic fields that affect the path of the electrons through the TEM. Because of this, the resolution of the TEM was limited to ~0.2 nm until middle of 1980s. Another important feature of the TEM is that it presents two-dimensional projections of three-dimensional specimens.

However, modern TEM are equipped with devices that allow for the aberration corrections, which made it possible for the researchers to achieve sub-Ångström resolution (~ 0.5-Å resolution at 300 keV). In fact, the highest-magnification image obtained using a transmission electron microscope has just been reported and has a resolution of 0.39 Å[35]. Consequently, a sensitivity of state-of-the-art TEM allows for imaging of individual atoms, which are of several Å in diameter, not

only in the bulk, but also in nano-systems[31]. Moreover, taking series of images each at different focus settings is believed to allow for a reconstruction of three-dimensional images [34].

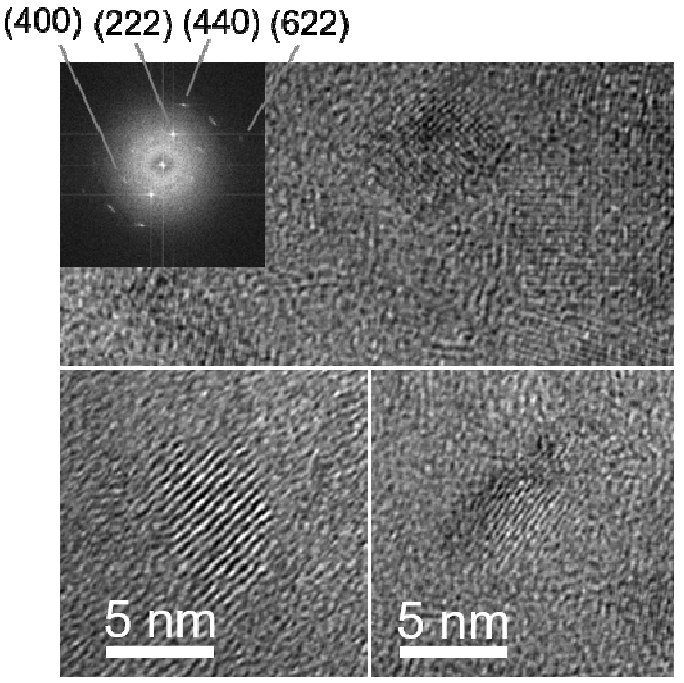

Figure 3.2 Transmission electron microscope images of pure Gd_2O_3 nanoparticles dialyzed for 1 day (lower left corner and upper overview), PEGylated Gd_2O_3 nanoparticles (GMP) (lower right corner) and a corresponding Fast Fourier Transform (FFT) for the PEGylated nanoparticles (GMP). For more discussion see Paper II.

TEM is efficient to study the size and crystallinity of nanoparticles samples. Figure 3.2 shows examples of TEM images of dialyzed Gd_2O_3 nanoparticles and Gd_2O_3 nanoparticles functionalized with PEG (PEGylated Gd_2O_3 nanoparticles) investigated in detail in Paper II. The former show crystalline particles. For the latter, it is possible to identify organic material, which is part of the samples. However, crystalline particles about 5 nm in size can still be found (Figure 3.2, the lower right corner). For further examples on Gd_2O_3 and Ce_2O_3 nanoparticles TEM studies, see previous works from group of Uvdal[15,29-30].

3.2. Dynamic light scattering

Highly efficient light scattering experimental technique that allows to study particles with ~1 nm in diameter is Dynamic Light Scattering (DLS), sometimes also called as Photon Correlation Spectroscopy or Quasi-Elastic Light Scattering). DLS is an optical method useful for studies of nanoparticles, allowing for the analysis of their dynamic properties and size distribution[36]. The basic set up of the DLS experiment is shown in Figure 3.3.

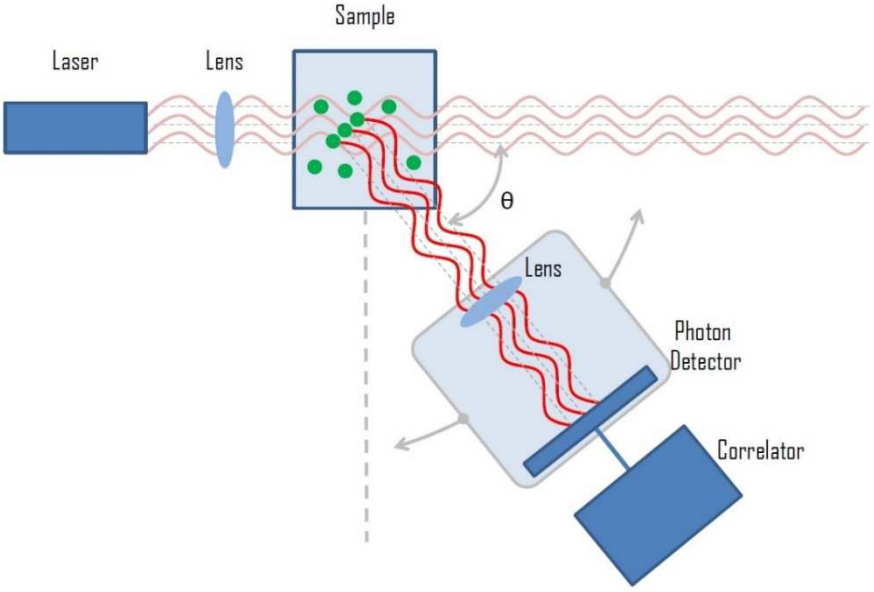

Figure 3.3 Schematic setup of Dynamic Light Scattering experiment.

A laser beam is used to illuminate a spatially limited volume within the sample, which for instance could be a colloidal suspension of nanoparticles. The latter scatter the light, and the information is obtained from time-dependent fluctuations of the scattered light. In principle, scattered light waves spread out in all directions with intensity $I_s(t)$, which is time-dependent. Indeed, nanoparticles in the colloidal suspension move randomly, or more correctly following the Brownian motion. Therefore, the interparticle distances fluctuate, leading to fluctuations of the phase relations of the scattered light. Moreover, the number of particles within the scattering region is not constant as a function of time:

some particles can enter or leave the illuminated part of the sample. Consequently, constructive or destructive interference of the scattering waves, is stochastic, leading to fluctuations of I_s. In DLS experiments, the fluctuations of I_s are detected at a known scattering angle θ by a fast photon detector (Figure 3.3).

In order to analyze the fluctuations of $I_s(t)$ one derives the so-called intensity correlation function $g_2(t)$. This can be done either by electronic digital correlator, that is using special hardware, or by software that performs statistical analysis of $I_s(t)$. From $g_2(t)$ it is possible to obtain the diffusion coefficient D of the particles. It is related to the hydrodynamic radius R of the particles via Stokes-Einstein equation[36]:

$$D=k_BT/(6\pi\eta R) \ , \qquad (3.1)$$

where k_B is the Boltzmann constant, T the temperature and η the viscosity.

The mean hydrodynamic radius R is the main parameter, which is determined from the most straight-forward DLS experiments. Note that modern advanced multi-angle instruments can be used to accurately determine the distribution of the particle sizes.

3.3. Infrared spectroscopy

Infrared vibrational spectroscopy allows one to identify molecules by analysis of vibrational properties of their constituent bonds. IR spectroscopy is an excellent tool for analyzing molecular structures. Relatively small systems can be studied, for instance, molecules adsorbed on metallic clusters[37]. IR spectroscopy can be used as an analytical tool of the surface composition and structure by making comparisons with surfaces of pure nanoclusters.

The infrared spectrum of a sample is recorded by passing a beam of infrared light through the sample, as shown schematically in Figure. 3.4a. The infrared light is used in the spectroscopy because it corresponds in energy to vibrational frequencies of most solids. There are two options to record the spectra. With the earliest spectrometers an IR spectrum could be measured by scanning the wavelength range using a monochromator. Today, the entire wavelength range is measured momentary. Then a transmittance or absorbance spectrum is generated by means of a Fourier transform instrument.

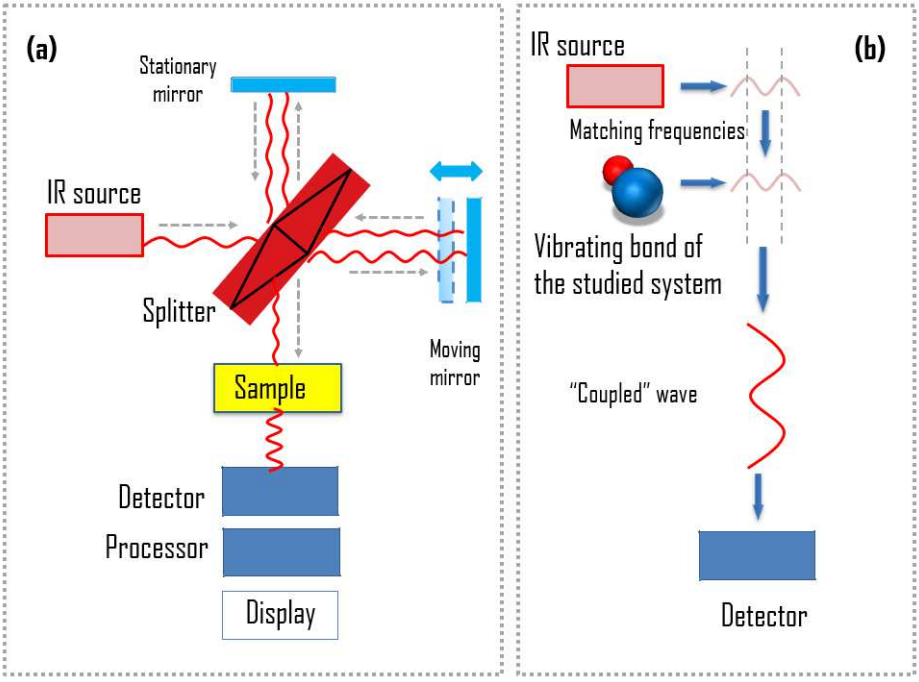

Figure 3.4 Schematic illustration of (a) setup of IR experiment and (b) physical principle behind the IR spectroscopy.

The physical principle behind the IR spectroscopy is illustrated in Figure 3.4(b). Each chemical bond in a studied system has its characteristic vibrational frequency (multiple modes are possible, of course, for group of atoms moving as a whole group). The technique is typically used for systems with covalent bonds. If the bonding in the system has an ionic component, vibrations of atoms lead to a modification of the dipole in the bond. Because of this, a photon with the frequency that matches the vibrational frequency will be absorbed by the system. The resonant frequencies are affected by the interactions between vibrating atoms, their masses, and the associated vibronic coupling. Therefore, analyzing the absorption spectra one sees how much energy was absorbed at each wavelength. In doing so one obtains valuable information about the chemical groups present in the sample, and consequently, about its composition.

Chapter 4

Hematopoietic cells for studies of nanoparticle-cell interaction

Biocompatibility of synthesized and characterized nanoparticles is vital for their use in medical applications, e.g. as MRI contrast agents. In general, evaluation of biocompatibility is a complex process that involves efforts from several disciplines, medicine, biology, chemistry and physics. A promising path on this route is to start with studies of nanoparticle interactions with isolated cells. In the present thesis several different cell types, e.g. neutrophil granulocytes and macrophages and their interaction with nanoparticles have been analyzed. The aim is to rule out in this way the nanoparticles which would be avoid for test animals prior to potential animal tests. Because of this, studies of nanoparticles interactions with individual cell types are useful for screening and in that sense much more efficient in comparison to animal tests when the task is to improve biocompatibility of the nanoparticles via functionalization, different types of synthesis, by capping or doping with other elements. Also, this approach allows for rapid feedback and speeding up the development of new nanomaterials.

All the cellular elements of the blood, including the cells of the immune system, arise from pluripotent hematopoietic stem cells in the bone marrow[38]. Division of the pluripotent cells produces two types of stem cells: a common lymphoid progenitor and a common myeloid progenitor. The former gives rise to the lymphoid lineage of white blood cells or leukocytes, which include the natural killer cells, as well as T and B lymphocytes. The latter gives rice to the myeloid lineage. The rest of leukocytes, including the monocytes, the dendritic cells and the granulocytes, as well as erythrocytes, and the megakaryocytes belong to the myeloid lineage. In this section I briefly describe cell types of interest for this study.

4.1. Polymorphonuclear neutrophils

Polymorphonuclear neutrophils (PMN) are a type of blood cells that belong to the granulocyte family of leukocytes. The granulocytes are characterized by multilobed nuclei and the presence of multiple, distinct granules within their cytoplasm. Besides neutrophils, the family also includes basophils and eosinophils[39]. PMNs develop and mature in the bone marrow from pluripotent CD34+ stem cells. The rate of production is ~5-10 x 10^{10} cells per day over a 7-14 days period[40]. The cells diameter within circulation is about 10 μm (see Figure 4.1). As a matter of fact, they are the most abundant circulating leukocytes in our blood. Indeed, the concentration of PMNs in the blood is ~2.5-7.5 x 10^9 cells/L. In the peripheral blood the concentration of PMNs is fairly constant if one deals with a resting uninfected host, because the production and elimination of the cells are balanced in this case. On the other hand, the lifespan of neutrophils in the circulation is quite short: their half-life is 7-12 hours. Neutrophils undergo spontaneous apoptosis before their removal by macrophage in the lung, spleen, and lever [40].

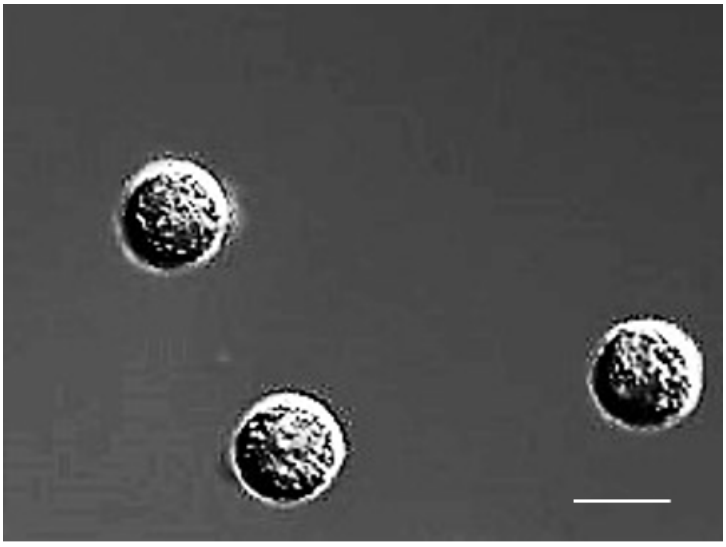

Figure 4.1 Differential interference contrast (DIC) microscopy pictures of human neutrophils. The scale bar indicates 10 μm.

At the same time, the number of circulating neutrophils increases greatly, up to an order of magnitude, during pathological conditions caused, for instance by a bacterial infection. Indeed, the PMNs act as the first defense of the immune system against invading pathogens. This property of the PMNs make them especially valuable for studies of effects of newly synthesized nanoparticles and their biocompatibility[41-43]. Indeed, PMNs represent a valuable model system to study a remarkable array of generalized cellular functions, as well as specialized functions and molecules important to host defense against infection, the mediation and resolution of inflammation[44]. Using the neutrophil model system, we may study several types of cellular process and biochemical pathways, including phagocytosis and oxygen radical production. Neutrophil activation by nanoparticles may lead to production and release of several different inflammatory mediators for example myeloperoxidase (MPO) into the extracellular space (into the buffer or medium). The cells may also express apoptosis (programmed cell death) and then for example shrink in size and express a lot of phosphatidylserine in their membrane[44]. The effects can be studied, e.g. by the cell clinic techniques.

4.2. Isolation of polymorphonuclear neutrophils from human blood

Isolation of PMNs from human blood employed in this work has been performed using a protocol adopted from the technique proposed by Böyum in 1968[45]. Its schematic representation is shown in Figure 4.2. Böyum proposed a technique for isolation of mononuclear cells from whole blood by one centrifugation, and of granulocytes by a two-steep procedure, combining centrifugation and a sedimentation. In short, anticoagulated blood was layered on top of a mixture of Isopaque and ficoll and centrifuged, and the cellular elements were divided into two main fractions. Granulocytes and erythrocytes sedimented to the bottom of the tube, while mononuclear cells and platelets remained at the interface. Diluting the blood with saline before the initial centrifugation, Böyum found truly remarkable efficiency of separation of the mononuclear cells, with almost 100% yield. At the second stage, mononuclear cells are removed and mixed the cell mass in the bottom of the tube with plasma and dextran. He removed plasma layer containing the granulocytes when erythrocytes had settled by sedimentation at 1 x g gravity field.

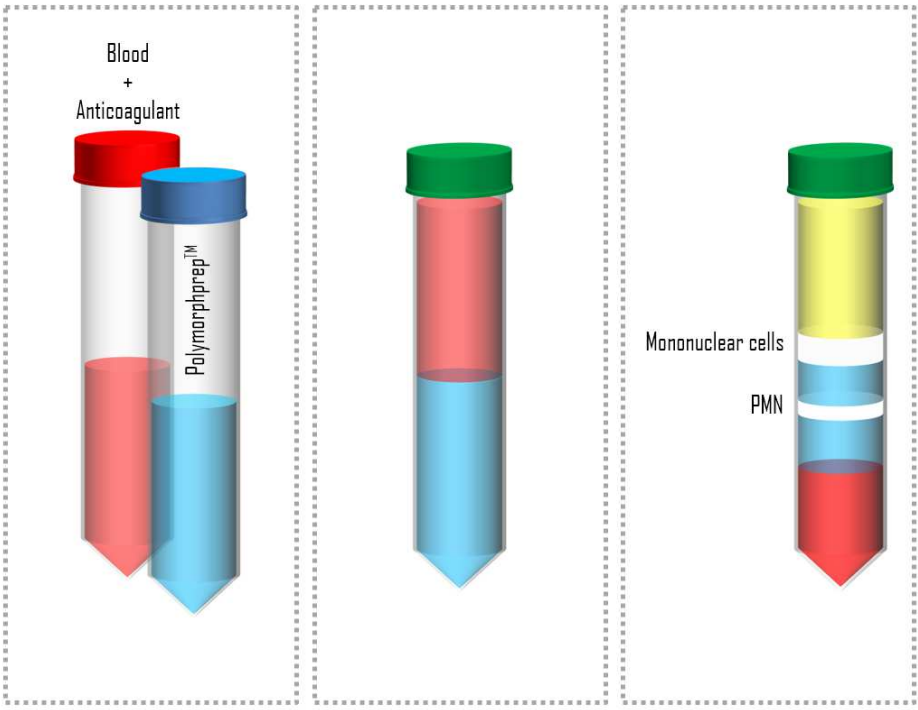

Figure 4.2 Schematic illustration of isolation of PMNs from human blood following the protocol employed in this work. See text below for further details.

In more details, the following protocol has been adopted in this work:

1. Prepare 25 ml venous whole blood donated by apparently healthy, non-medicated volunteers. Blood must be anti-coagulated with 10U/ml heparin and must be allowed to equilibrate to room temperature.
2. Layer the blood on an equal volume of a density gradient (Polymorphprep ™, see Figure 4.2, middle panel)
3. Centrifuge at 480 x g for 40 min at room temperature. Allow the rotor to decelerate with very weak braking.
4. Remove the top layer (plasma), the second layer (mononuclear cells) and the third layer (remained Polymorphprep™), see Figure 4.2, right panel. Harvest the next layer (the lower band of PMNs) into a new 50 ml centrifuge tube.

5. Resuspend the harvested material with an equal volume of 0.45% NaCl solution. Add ca 20 ml of PBS equilibrated to room temperature. Turn the tube couple of times.
6. Centrifuge at 400 x g for 10 min at room temperature.
7. Pour off the supernatant to harvest the PMNs and resuspend the pellet carefully.
8. Remove residual erythrocytes by brief (35 s) hypotonic lysis in 4.5 ml cold distilled water. Then add 1.5 ml PBS containing 3.4% NaCl. Next add 5 ml cold Hepes-buffer. All operations of (8) must be done on ice.
9. Centrifuge at 400 x g for 5 min at temperature $+4^0$C.
10. Repeat operations described in (7)-(9).
11. Pour off the supernatant and resuspend the pellet carefully. Add 1 ml ice-cold Hepes-buffer. Take 10 µl of the cell suspension for a cell counting.
12. Dilute the cell suspension in Hepes-buffer to a needed concentration, in this work usually to $2*10^6$ cells/ml.

4.3. ROS production

PMNs are phagocytic cells of the innate immune system. Although traditionally considered as an innate immune cell, recent knowledge points towards a more complex role of these cells also involved in chronic inflammatory processes and as a contributor in adaptive immune responses. Clearly, they are potent cells capable of releasing for example a range of immunomodulatory molecules[46].

They react first to defend the host against invading pathogens, mainly bacteria and fungi, but also viruses[40]. PMNs have powerful microbicidal equipment, and they have been shown to play a large role in inflammatory responses. For instance, neutrophils react quickly, within minutes to an hour of tissue injury, making themselves into a hallmark of acute inflammation. They are mobile, and they have a capacity to seek and destroy different targets following phagocytosis of an invading pathogen. Neutrophils at rest consume relatively small amounts of oxygen. However, in case of an agonist challenge, their consumption of oxygen increases dramatically. Neutrophils reduce oxygen to superoxide anions O_2^- through the activation of the enzymatic system which is unique for phagocytic cells, including neutrophils. Specifically, the process is mediated by nicotinamide adenine dinucleotide phosphate

(NADPH)-oxidase enzyme. The superoxide anions could further metabolize to hydrogen peroxide (H_2O_2) and other even more toxic substances. O_2^-, H_2O_2, singlet oxygen, and other products derived from the metabolism of H_2O_2 generated by neutrophils following the uptake of particles or in response to inflammatory stimuli are referred to as reactive oxygen species (ROS). The process described above is also referred to as "the respiratory burst" defined as an increase in the oxidative metabolism[40].

Moreover, the neutrophils antimicrobial activity essential for pathogen killing also involves the release of their intracellular granules, in addition to ROS production. The granules contain lytic enzymes and antimicrobial polypeptides. At the same time, it is worth to point out that PMNs-derived respiratory burst could damage the surrounding tissues upon uncontrolled release of ROS. In fact, there are inflammatory diseases dominated by neutrophils. Therefore, neutrophils turnover should be controlled quite strictly.

To measure the ROS production, one can use the effect of chemiluminescence. Indeed, simultaneously with generation of oxidative metabolites by neutrophils upon the respiratory burst, the light is also generated, that is the chemiluminescence takes place. The light can be detected, and the sensitivity of the measurements can be increased via addition of luminol or 2,7-dichlorofluorescein diacetate (DCF-DA, Sigma Aldrich, St Louis, MO, USA). Both substances can be excited by ROS, and then emit photons upon the transition to the ground state. The molecules can pass the biological membrane, and therefore they can be used for the measurements of both, intracellular and released oxygen radicals. However, if one needs to measure only released oxygen metabolites, it is possible to use isoluminol, which does not penetrate cells because of its chemical structure.

An example of chemiluminescence recordings of the reactive oxygen species (ROS) production from neutrophil granulocytes from Paper I is shown in Figure 4.3. Neutrophil granulocytes ($2x10^6$ cells/ml) were challenged with IgG-opsonized yeast particles ($5x10^6$ yeast particles/ml) after an initial exposure to as synthesized Gd_2O_3 nanoparticles (0.94 mM) for 15 minutes. Results obtained on control cells with only IgG-opsonized yeast are shown for comparison. Chemiluminescence was recorded, using luminol, in a Microplate Fluorescence Reader FL600. The ROS production was calculated as relative chemiluminescence in-

tensity in percentage of control cells treated only with IgG-opsonized yeast particles.

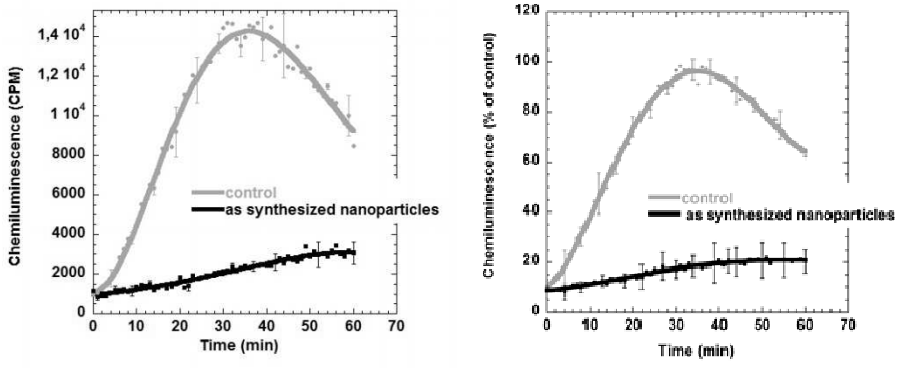

Figure 4.3 Chemiluminescence recordings of the reactive oxygen species (ROS) production from neutrophil granulocytes challenged with IgG-opsonized yeast particles after an initial exposure to as synthesized Gd_2O_3 nanoparticles (black lines). Gray traces show chemiluminescence from control cells with only IgG-opsonized yeast. Mean ± SD of one representative experiment (in counts per minute, CPM) and taken from three different donors (as % of control), all run in duplicate are shown in panels left and right, respectively. In both panels the circles represent the mean values, and the lines connecting them are results of the 5-th order polynomial fit between the data points. Republished with permission of IOP Publishing, from Paper I; permission conveyed through Copyright Clearance Center, Inc.

4.4. Macrophages

Monocytes circulate in the blood and continuously migrate into tissues where they differentiate to macrophages[38]. Macrophages represent the mature form of monocytes, resident in almost all the tissues where they may be relatively long-lived cells. Because most infections occur in tissue, macrophages are the primary cells that perform important protective function of first defense in innate immunity. Their functions include:

- to engulf and to kill invading microorganisms;

- to secrete signaling proteins that activate other immune system cells and to recruit them into an immune response;
- to act as general scavenger cells in the body, cleaning dead cells and cell debris.

In particular, the pulmonary-alveolar macrophage (PAM) is the resident mononuclear phagocyte of the lung and functions as the primary defense against inhaled particulate matter. The study of these cells in animals started in early 1960s with a description of a procedure to obtain rabbit PAMs via lung washings. The retrieval of human PAMs became possible with the development of the bronchopulmonary-lavage technic in men. Fiberoptic bronchoscopy has transformed recovery of alveolar macrophages in many diseases into a routine procedure leading to improved diagnosis[47].

On the other hand, investigations of the immunological functions of PAM cells in small laboratory animals has been impeded by the relatively low number of AMs recoverable by bronchopulmonary-lavage techniques. A supply of homogeneous cells in significant quantity has been achieved through the establishment of continuous cultures of murine peritoneal macrophages that retain many of the characteristics of the macrophages recovered directly from animals. Mbawuike and Herscowitz described the establishment, growth characteristics, and functional activity of a continuous line of alveolar macrophages derived from bronchoalveolar lavage cells obtained from Balb c/J mice[48]. In Paper VI, we used an immortalized murine alveolar macrophage cell line (MH-S)[48] to investigate the optimization of the cell uptake and to examine the potential of new intracellular contrast agent for magnetic resonance imaging.

4.5. THP-1 cells

THP-1 cells are derived from a human monocytic leukemia cell line. THP-I cells differentiate into macrophage-like cells following a treatment with phorbol esters. These cells mimic native monocyte-derived macrophages. Access to large amounts human monocytes may be limited and thus the THP-1 cell line may be a good option for initial *in vitro* studies. Compared to other human myeloid cell lines, differentiated THP-I cells show a behavior similar to that of native monocyte-derived macrophages. It resembles the human monocyte with respect to numerous criteria such as morphology, secretory products, oncogene

expression, expression of membrane antigens, and expression of genes involved in lipid metabolism. Moreover, an additional advantage of a cell line THP-1 in comparison with native human monocytes is a homogeneous population, which facilitates biochemical studies[49].

4.6. BA/F3 cells

Ba/F3 is a murine bone marrow-derived cell line dependent on interleukin 3 (IL-3) dependent hematopoietic cell for viability and proliferation[50]. Ba/F3 cells are classified as early cells of the lymphoblastoid lineage by virtue of their low-level expression of the B-cell-specific B220 antigen and the germ-line configuration of their immunoglobulin loci. The cells are able to grow in medium supplemented with fetal calf serum and purified recombinant IL-3 alone. However, in the absence of an exogenous source of IL-3, Ba/F3 cells fail to proliferate and rapidly die. Details of culturing and labeling of BA/F3 cells are presented in Paper III.

Chapter 5

Techniques for studies of cell-nanoparticle interactions

5.1. Magnetic resonance imaging

Magnetic resonance imaging, or MRI, is a powerful medical technique. It provides strikingly clear pictures of almost all organs of the body, such as the brain, the spinal cord and lungs. The technique is based on discoveries made by physicists in the first half of last century.

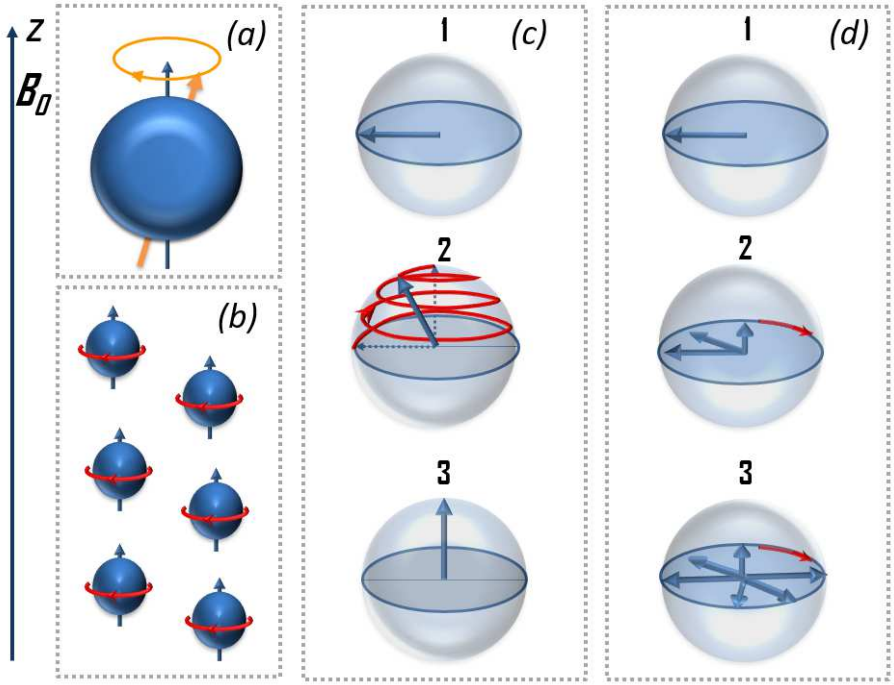

Figure 5.1 Basic idea of NMR experiment. (a) Magnetic moments (nuclear spins) precess about axis of the external static magnetic field B_0. (b) Alignment of nuclear spin moments in the static magnetic field. (c) Longitudinal relaxation. (d) Transverse relaxation. See text for more discussion.

In 1938 the effect was discovered by Isidor I. Rabi, who introduced the name of the technique known now as nuclear magnetic resonance (NMR)[51]. The experiments were done on atomic beams of silver atoms. Rabi was awarded the Nobel Prize in physics in 1944 for the discovery. In the late 1940s, Edward Purcell[52] and Felix Bloch[53-54] observed the effect on protons in paraffin and in water, respectively. They shared the Nobel Prize in Physics 1952 "for their development of new methods for nuclear magnetic precision measurements and discoveries in connection therewith". The principal reason for the effect is related to the fact that some atomic nuclei, e.g. hydrogen protons, behave like magnets (Figure 5.1(a)). Thus, they can be aligned in the external magnetic fields and perturbed by electromagnetic waves.

The basic idea of the NMR is shown in Figure 5.1. Consider a system of atoms in a magnetic field B_0. Their magnetic moments (nuclear spins) should precess about the external field axis (Figure. 5.1(a)), orienting parallel to the field. This leads to a magnetic polarization in the direction of the magnetic field, which is often denoted as the z direction (Figure. 5.1(b)). Consider next an oscillating magnetic field with frequency ω applied in the perpendicular direction (x or y). If ω and B correspond to a resonance condition:

$$|\gamma|B_0 = \omega \quad , \tag{5.1}$$

where γ is a constant for a given isotope (the so-called gyromagnetic ratio), the nuclear spins are deflected from the original z direction. Upon the excitation, the magnetic polarization vector of the nuclei rotates in a plane perpendicular to the z axis (Figure 5.1(c) and (d)) inducing an electromagnetic field in a detector coil. The detected field is the NMR signal[55].

Of primary importance for imaging is the return of nuclear spins to equilibrium, that is to their original orientations parallel to the static applied field B_0, called the nuclear magnetic relaxation. One distinguishes the longitudinal relaxation along the z-direction (Figure. 5.1(c)). and transverse relaxation in xy-directions (Figure. 5.1(d)). Let us denote the time of the excitation τ as 0. The number of moments parallel to z-direction is minimal at τ=0 (moments rotate in xy-plane). When they start to “return” to the direction of the magnetic field B, and the time dependence of magnetization M_z in z-direction behaves like:

$$M_z(\tau) = M_z(0)(1\text{-}e^{-\tau/T_1}) \qquad (5.2)$$

(see Figure 5.2). This longitudinal relaxation reflects a loss of energy, as heat, from the system to its surrounding ("lattice") and is primarily a measure of the dipolar coupling of the proton moments to their surroundings[56]. The constant T_1 characterize the spin-lattice relaxation time: it is the time for the longitudinal magnetization M_z to reach 63.212 % (factor $1\text{-}e^{-1}$) of the maximal values of longitudinal magnetization M_0.

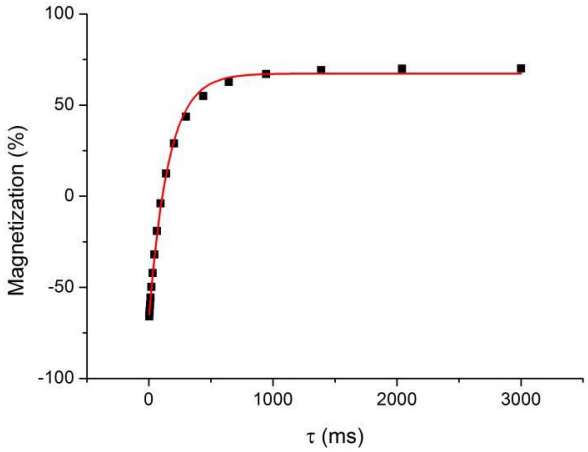

Figure 5.2 Time dependence of longitudinal magnetization M_z measured using Bruker minispec low-field pulsed NMR spectrometer.

In addition to the longitudinal relaxation, there is a transverse relaxation. At τ=0 moments rotate in *xy*-plane in phase with each other, corresponding to maximal value of the signal. With time the dephasing takes place, and the signal decreases. Time dependence of transverse magnetization M_{xy} in *xy*-plane behaves like:

$$M_{xy}(\tau) = M_{xy}(0)e^{-\tau/T_2} \qquad (5.3)$$

(see Figure 5.3). The constant T_2 characterizes the return of M_{xy} to equilibrium. It is called the spin-spin relaxation time and corresponds to time at which the transverse magnetization M_{xy} is reduced by a factor of e^{-1}, what is to 36,788% of the maximal value of the magnetization.

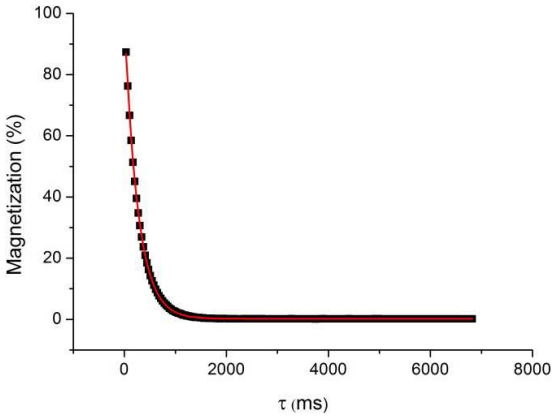

Figure 5.3 Time dependence of transverse magnetization M_{xy} measured using Bruker minispec low-field pulsed NMR spectrometer.

The detected NMR signal is specific for each type of the atoms. For example, characteristic NMR signals from the hydrogen atoms can be detected quite efficiently. Moreover, the outcome of the NMR experiment depends on the surrounding of the atoms. Thus, the NMR has been successfully used to investigate the structural properties of materials. It is very important that for hydrogen nuclei in liquids T_1 is of the order of seconds (Figure 5.2), because it determines the time of the measurement. If instead of seconds it would take hours for the spins to repolarize, the NMR technique would be impractical for MRI[55]. T_2 is on the order of hundreds of milliseconds (Figure 5.3), and it determines the sharpness of the resonance.

Water that makes up most of the content of our cells is the abundant source of hydrogen. In 1973 Paul Lauterbur showed how these could be viewed using NMR signals[57]. As a matter of fact, NMR was used for biological applications earlier. In 1971, Raymond Damadian observed that some malignant tissue, obtained from implanted tumors removed from rats, had longer NMR relaxation times than many normal tissues. The observation received attention in medical community, but the experiments were carried out at rats, which were dissected, and the tissue samples studied by NMR. Lauterbur, who was the chemist, not ordinarily involved with animal experiments happened to observe the entire process and found them rather distasteful[58].

He started to search for the methodology in which the signal intensities, relaxation times, etc., could be measured from outside the living body with sufficient spatial resolution[58]. He intentionally introduced small gradients in the strength of the magnetic field. Using thin-walled glass capillaries of water (H_2O) attached to the inside wall of glass tube of heavy water (D_2O), he showed that it is possible to distinguish hydrogen nuclei in different parts of a sample. Lauterbur combined the signal recorded with gradients applied in different directions through a sample, and constructed images that gave the spatial locations of hydrogen nuclei[57].

The discovery laid the ground for medical applications of NMR, the MRI. However, it took time to develop the idea that showed a possibility to identify the contents of a test tube to visualize the contents of human bodies. Very important step was taken by Peter Mansfield who developed the scheme known as echoplanar imaging[59]. The scheme improved the resolution and speed of MRI to such an extent that it takes seconds rather than hours to take an image. The discovery of the MRI led to Nobel Prize in Physiology and Medicine awarded to Paul C. Lauterbur and Peter Mansfield in 2003[60].

MRI has become a routine diagnostic tool in modern clinical medicine. Its advantages as a diagnostic imaging modality are as follows: [61]

- it is noninvasive;
- it delivers no radiation burden;
- it has excellent (submillimeter) spatial resolution;
- soft tissue contrast is superb;
- anatomical information yields readily.

Importantly, different realizations of MRI can provide contrast with quite different images from the same anatomical region, highlighting differences in proton density, T_1 or T_2 relaxation times. In fact, the image contrast in MRI can be classified according to its sensitivity to these three parameters. A sequence that is mainly sensitive to the first of the parameters is called a proton-density-weighted image, while image sequences that are mainly sensitive to T_1 or T_2 relaxation times, are called T_1 or T_2-weighted images, respectively[62].

Unfortunately, the sensitivity of MRI is relatively low, which represent one of the major challenges for the applications. Perhaps the most promising way to improve the sensitivity is to use the so-called MRI contrast agents, substances that affect property of water protons to such

an extent that an observable effect leads to enhanced contrast[61]. The detailed discussion of contrast agents is given in Ch. 6.

5.2. Morphological studies of cell-nanoparticle interactions using fluorescence microscopy

The term "fluorescence" was introduced by Friedrich Mohs, who in 1824 observed light from heated fluorite[63]. 9 years later, Sir David Brewster used the lens to condense sunlight into a chlorophyll solution and observed bright red emission in response. Still, the discovery of the fluorescence is credited to Sir George Stokes (1852), who in addition to observation of a strong photoluminescence from fluorite under UV light, also explained the effect.

Nowadays, the fluorescence microscopy became an efficient technique for the morphological examination of cells that is often used to evaluate inflammatory response induced by nanoparticles. It allows one to visualize different compartments of the cells stained with appropriate fluorescent molecules. For instance, neutrophils can be stained for filamentous actin, e.g. with BODIPY®FL phallacidin (Paper I), and become better observed against the dark background, allowing for substantially more accurate examination of the cell morphology, including pseudopodial activity, as well as their aggregation.

Fluorescence microscopy is a tool for obtaining a magnified image of an object employing the luminescence of excited atoms or molecules of the studied object. A luminescent material absorbs energy at moderate temperature, and then re-emits part of it as IR, visible or UV light[63]. The latter is used to measure the ROS production, as described in Sec 4.3 above.

A simple picture that illustrate the modern understanding of the fluorescence is presented in Figure 5.4. Upon the absorption of energy hv carried by a photon with frequency v, an electron in the luminescent material is excited from an occupied state into an unoccupied state, leaving the hole behind. Subsequently, the electron and the hole recombine, emitting the photon hv'. The emitted light is shifted to longer wave length, so the frequency of the emitted photon $v' < v$. The difference (in wavelength) between the absorption and emission peak is called Stokes shift. For instance, if the blue light is used for the excitation, the emitted light can be green. Note that in fluorescence the emission of light by the luminescent material stops as the excitation stops.

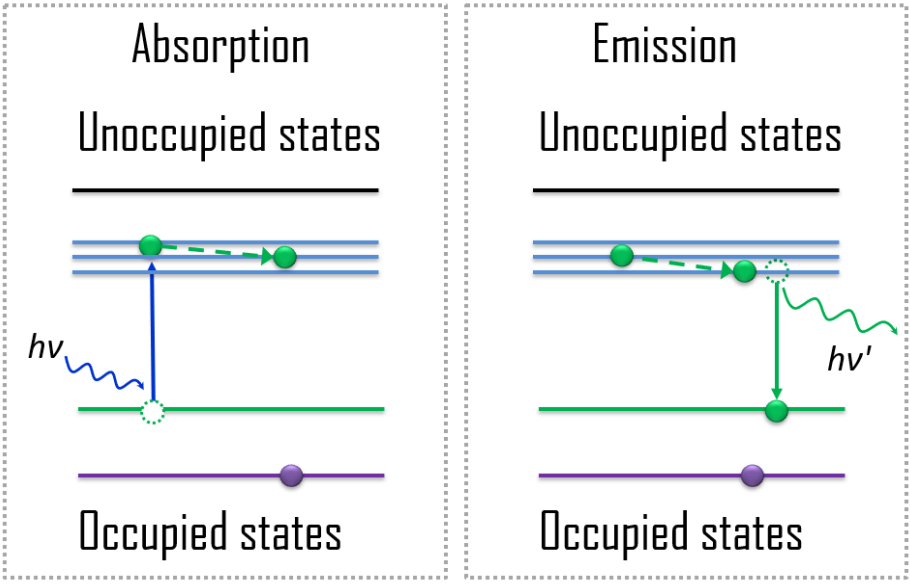

Figure 5.4 Schematic illustration of fluorescence. Energy states of the luminescent material are shown with solid lines. The low-lying energy states are occupied, the higher energy states are unoccupied. Electrons are shown as filled circles, holes are shown by empty circles, photons are shown with arrows. See text for more discussion.

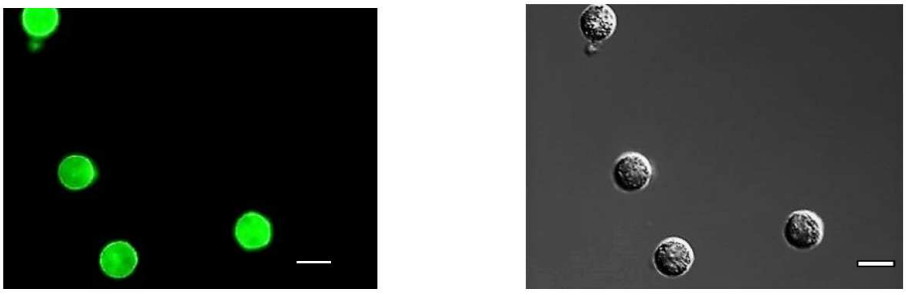

Figure 5.5 Comparison of fluorescence (left) and differential interference contrast (DIC) microscopy images of human neutrophils (right) microscopy images of unstimulated neutrophil granulocytes. The scale bars indicate 10 µm.

The fluorescence microscopy has number of important advantages which makes it into a powerful tool in cell and molecular biological research. Moreover, it is possible to use different fluorophores to track different parts of the cells, contributing to high selectivity of the technique. The enhanced features of the fluorescence microscopy as compared to the (normal) light microscope can be seen in Figure 5.5, where light and fluorescence microscopy images of unstimulated neutrophil granulocytes are compared. Note that the fluorescence images can be superimposed on light images for even more information[64].

The strength of the fluorescence microscopy in studies of nanoparticles-cells interactions is demonstrated in Figure 5.6. It compares images of neutrophil granulocytes exposed to as prepared Gd_2O_3 nanoparticles and to functionalized (PEGylated) Gd_2O_3 nanoparticles, which will be discussed in detail in Sec. 6.4 and Ch. 7, respectively. Recalling that unstimulated neutrophils show a round morphology (Figure 5.5), one sees a clear change in cell morphology for neutrophils exposed to as prepared Gd_2O_3 nanoparticles. Enhanced fluorescence intensity close to the cell walls, due to reorganization of actin is clearly seen: neutrophils form pseudopodia (extensions), spread, and become polarized. On the contrary, there is no such activation when the cells are exposed to PEGylated Gd_2O_3 nanoparticles. The spherical shape of the cells and the homogeneous intensity indicate that the neutrophils are at rest. The comparison shows that this integral part of the immune system was not activated by functionalized (PEGylated) Gd_2O_3 nanoparticles. The positive effect of the functionalization will be further discussed in Chapter 7.

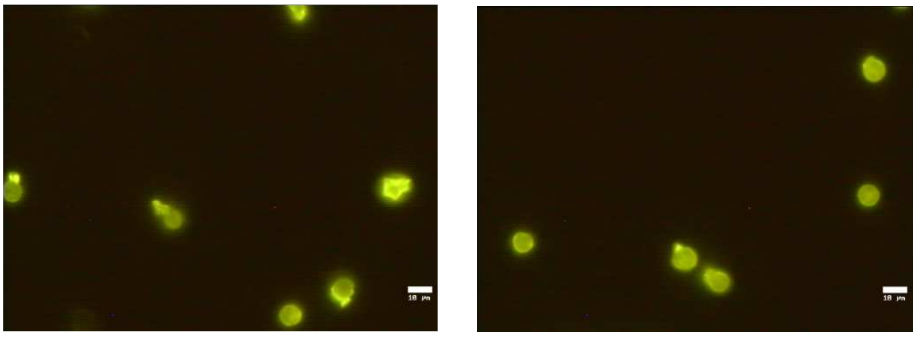

Figure 5.6 Fluorescent microscopy images of neutrophil granulocytes exposed to as prepared Gd_2O_3 nanoparticles (left) and to functionalized (PEGylated) Gd_2O_3 nanoparticles (right).

5.3. Capacitive sensors based on Lab-on-a-chip technology

Development of new nanoparticles for biomedical applications will strongly benefit from cost-effective, portable and technically efficient methods for evaluating studies of cell-particle interactions. Indeed, monitoring cells and cell activation during external triggers are of main importance for increased understanding of the mechanistic processes of cells and foreign elements. A possibility to view and follow processes without disturbing the studied system by the measurement itself is an important goal of on-going development of novel measurement technologies. In this respect, an ideal biosensing systems should represent non-invasive, label-free, real-time, and data-rich measurement technology. Biosensors measure electrical, optical, magnetic, or mass related properties of biological samples, and interest in the technology grows rapidly[9]. Different physical phenomena have been suggested for the sensing, like surface plasmon resonance spectroscopy[65], optical sensing[66], and electrochemical sensing.

One well-known example of the latter is the impedance measurement of live biological cells. It is widely accepted as an easy-to-use quantitative analytical method to assess cell status, flexible for device design and fabrication. The measurement of the impedance, which is the complex ratio of the voltage to the current in an alternating/direct current circuit is realized in three typical techniques: electric cell-substrate impedance sensing, impedance flow cytometry and electric impedance spectroscopy[67]. Unfortunately, upon the impedance measurements the cells are typically in direct contact with the electrodes and thus subjected to an electric current flow due the electrically conductive cell media. This, as well as possible uncontrolled electrochemical reactions and electrode corrosion represent the main drawbacks of the approach.

An alternative electrochemical technique to study cells adhering onto a substrate, which has been developed more recently is based on capacitive sensing[68]. The basic idea of the sensing in this approach is that upon activation of cells their morphology changes and ROS are released, which can be monitored through relative capacity change. Importantly, the measurements can be made in such a way as to avoid a direct electrical contact to the cells.

Combining computation and sensing capabilities offered by complementary metal oxide semiconductor (CMOS) has led to a design of novel Lab-on-a-chip (LOC) devices with a potential to replace large-scale

laboratory equipment[9,68]. The CMOS/ Low temperature co-fired ceramic (CMOS/LTCC) devices of that type have been employed in this study to monitor activity of just a few cells minute by minute. The method is purely capacitive, and it avoids a direct contact of electrodes with the cells. It enables continuous monitoring of cell adhesion, morphological changes, ROS production and possibly adhesion and detachment processes with high time resolution and from just a few cells in a non-invasive way. Below we outline main ideas of the method and show results that demonstrate capability of a novel informationally dense non-invasive methodology to monitor neutrophils at work. Detailed presentation of the technique and obtained results is given in Paper V.

Schematic representation of CMOS/LTCC device for measurement of neutrophils activity is presented in Figure 5.7. Each interdigitated sensing electrode is positioned underneath the top layer of oxide with electrode area of 30 µm x30 µm. It is connected to one stage of a three-stage ring oscillator. Sensor capacitance is adjusted so that oscillation frequency is ~60MHz when the surface of the sensor is clean. Adhesion of neutrophils to the surface and their activity, e.g. upon the oxidative burst or exposure to PMA (Figure 5.8) result in a change of the dielectric constant in the proximity of sensor surface, leading to the change of the capacitance, which is related to the effective permittivity of the sample. Consequently, the oscillation frequency of the circuit increases when effective permittivity is lowered and vice versa. The results can be plotted at the computer in the dependence of frequency on measurement time (Figure 5.9).

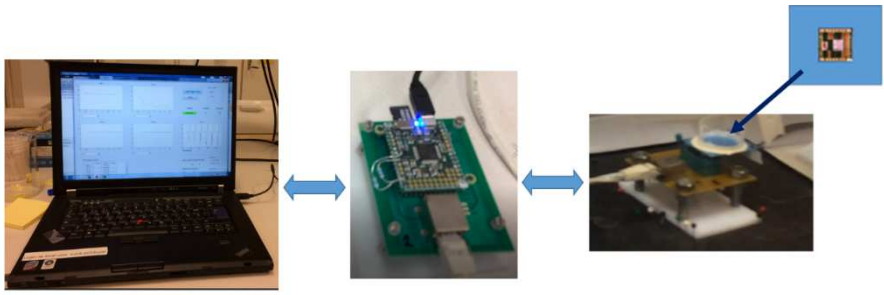

Figure 5.7 Schematic representation of CMOS/LTCC device for measurement of neutrophils activity. Computer, microcontroller and sensor chip module are shown from left to right. Sensor chip is shown as inset.

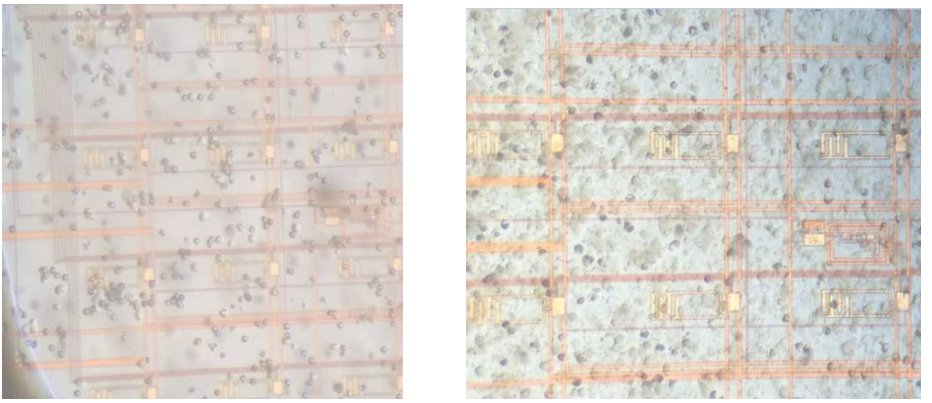

Figure 5.8 Microscope image of the sensors on the part of the chip. Left panel shows sensors exposed to the medium after unstimulated neutrophils have been added. Right panel shows sensors with neutrophils stimulated with PMA.

In Figure 5.9 response of CMOS/LTCC device on treatment of neutrophils with PMA is demonstrated. Neutrophils were attached to CMOS sensor and incubated for 30 min in 37°C under soft shaking. At 30^{th} minute of the experiment 15 µl of 1mM PMA was added, and during the next 20 min we see that neutrophils clearly react. The media surrounding the cells is changing when the ions are released from the activated cells.

Therefore, the ionic conductivity became dominating factor that determined the change of the sensor output frequency. Ions released to the liquid accumulate on the sensor surface above the electrode, leading to increase of effective permittivity (see Paper V). Capacitance of the cells suspension changes and the frequency detected by the sensors drops gradually from level before stimulation (taken as zero for all sensors) to final state. The decrease of the frequency can be viewed as a proof-of-concept that the capacitive sensors based on Lab-on-a-chip technology are indeed capable to monitor neutrophils activity.

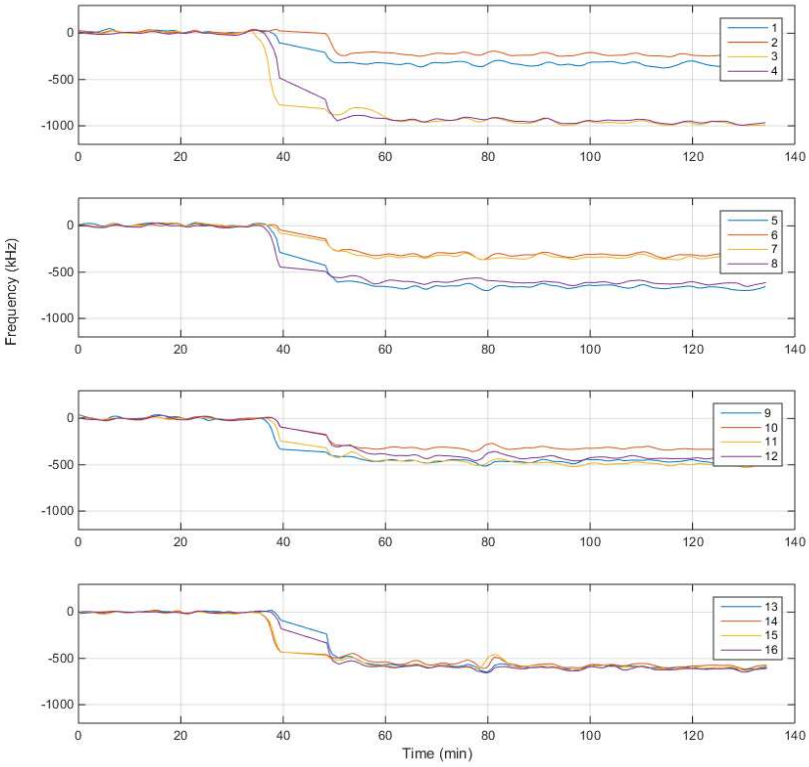

Figure 5.9 Response of CMOS/LTCC device on treatment of neutrophils with PMA. See text for detailed discussion. The baseline has been normalized to 0 for all sensors.

Chapter 6

Nanoparticles as MRI contrast agents

6.1. General considerations

Large range of relaxation times found for the water protons in mammalian tissues-from about 100 ms to several seconds is the basis of MRI contrast. The contrast in MRI is a continuum, and unlike in medical X-ray imaging, there is no universal gray scale. Moreover, in most diseased tissues, such as tumors, the relaxation times are prolonged. This difference provides the basis for image contrast between normal and pathological tissues[55]. Moreover, the relaxation times T_1 and T_2 can be affected, in fact decreased, by the use of a magnetic nanoparticles as contrast agent. Because it was demonstrated that tumor cells relaxation times were not altered by the contrast agents, their use allowed for identification of different kinds of tumors, like brain tumors[69] and liver tumors[70] .

MRI contrast agents can be defined as a unique class of pharmaceuticals that enhance the image contrast between normal and diseased tissue and indicate the status of organ function or blood flow after administration by increasing the relaxation rates of water protons in tissue in which the agent accumulates[62]. The ability of a contrast agent to change a relaxation rate is quantified in terms of parameters called relaxivity[61]. Relaxivity parameter r_1 is related to the longitudinal relaxation time T_1 as

$$r_1 = \frac{\Delta(1/T_1)}{M} \quad , \tag{6.1}$$

where $\Delta(1/T_1)$ is the change in relaxation rate after the introduction of the contrast agent, and M denotes the concentration of the contrast agent. Similarly, relaxivity r_2 is related to the transverse rate, given by inverse relaxation time T_2.

At present, the most common contrast agents are paramagnetic gadolinium ion complexes, which will be discussed in Sec. 6.3. At the same time, superparamagnetic nanoparticles are commercially available, such as ‘Feridex I. V.’, an iron oxide contrast agent marketed by Advanced

Magnetics Inc. for the organ-specific targeting of liver lesions[56]. The available contrast agents can be categorized according to their influence on the relaxivity parameters into so-called T_1-agents and T_2-agents. The former generally decrease the longitudinal relaxation times (or increase the longitudinal relaxation rates) of water protons in tissue more than the transverse relaxation times (or rates)[62], and are sometimes referred to as positive contrast agents. Since T_1-agents enhance the relaxation rate to the surrounding media on short distance, they enhance signals in all parts of the sample with a short relaxation time T_1 and suppresses it in the parts of the sample with a long T_1 relaxation time. Paramagnetic gadolinium-based contrast agents belong to this class. T_2-agents can be called negative contrast agents, and include, for instance, ferromagnetic iron oxide particles.

Several requirement for MRI contrast agent have been formulated[62]:
- high relaxivity and specificity;
- low toxicity and side effects;
- suitable long intravascular duration and excretion time;
- high contrast enhancement with low dose in vivo;
- low cost.

Design of novel contrast agents is highly important, but a challenging task. The aim for development is to find novel compounds with improved relaxivity that can be detected at lower doses, as well as compounds that can provide greater contrast at equivalent doses to compounds with lower relaxivity. Below we briefly discuss the available contrast agents, followed by more detailed description of novel Gd_2O_3-based nanoparticles, which are the main subject of the present thesis.

6.2. Fe-oxide based contrast agents

Iron oxide nanoparticles were the most commonly used superparamagnetic contrast agents. The ferrite colloids, magnetite (Fe_3O_4) and maghemite (γ-Fe_2O_3) are two types of the magnetic nanoparticles that were considered in the medical and pharmaceutical fields. They were thought to be sufficiently biocompatible, and their biodegradability was believed to be efficient[16]. Moreover, dextran coated iron oxides could be excreted via the liver after the treatment. The particles are selectively taken up by the reticuloendothelial system, a network of cells lining blood vessels whose function is to remove foreign substances from the bloodstream[56].

In this respect, the size of the nanoparticles is very important. If the diameters of the particles are above 30 nm, they are rapidly collected by the liver and spleen. On the contrary, the nanoparticles of less than 10 nm are collected by reticuloendothelial cells throughout the body, including those in the lymph nodes and bone marrow[71]. According to Ref.[19], particles with a diameter ranging from 10 to 100 nm were considered as optimal for intravenous injection and had the most prolonged blood circulation times.

Applications of Fe-oxides based nanoparticles have been extensively reviewed[19,56]. As examples, successful targeting of the endothelial inflammatory adhesion molecule E-selectin by MRI in the context of *in vitro* and *in vivo* models of inflammation, specific cell tracking *in vivo* by MRI, and the development of a biostable methotrexate-immobilized iron oxide nanoparticle drug carrier that may potentially be used for real-time monitoring of drug delivery through MRI were mentioned. In addition, successful use of Fe-oxide nanoparticles for magnetic cell separation and magnetic drug targeting were pointed out. Magnetic nanoparticles have also been utilized for the *in vivo* monitoring of gene expression, a process in which cells are engineered to overexpress a given gene and in selectively studies of cells that were in the process of cell death.

Unfortunately, there are several disadvantages in using the superparamagnetic Fe-oxide-based contrast agents. The key factors named in this respect in the literature are related to a negative contrast effect and magnetic susceptibility artifacts[72]. The dark signal in T_2-weighted MRI could be confused with the signals from bleeding, calcification or metal deposits and consequently mislead the clinical. The susceptibility artifacts distort the background image. T_1 contrast agents do not have such disadvantages, and they may be more beneficial for high-resolution imaging. Recently, we have shown that we can obtain Fe_2O_3 nanoparticles with positive contrast by nanomaterial design, i.e. scaling down in size, see our first results[11,13].

6.3. Gd chelates based contrast agents

Gd is a lanthanide metal. Its Gd^{3+} ions have seven unpaired electrons, tensuring high value of local magnetic moment, the symmetric electronic states and high relaxivity. Its high magnetic properties are highly beneficial for the use as MRI contrast agent, but unfortunately, it cannot

be used in the ionic form due to the undesirable biodistribution and relatively high toxicity[62]. The point is that the lanthanides in general are non-toxic, because they cannot cross cell membranes and are therefore not absorbed if ingested orally[20]. After intravenous administration the lanthanides are cleared from the blood and redistributed to tissues, primarily the liver and bone. The process occurs quite rapidly. At the same time, they gain access to cells expressing calcium channels if they are administrated by that route. This could lead to acute toxicity: a drop in blood pressure followed by cardiovascular collapse and pulmonary paralysis. Moreover, chronic toxicity is generally associated with hepatotoxicity and edema[20].

On the other hand, Gd^{3+} ions may be introduced into the body after having been chelated to a ligand. The ligands used for complexing should have a strong and specific affinity for the active ingredient. The aim is to make the complexes stable in the body and that they should be excreted intact. Using acyclic and macrocylic polyaminocarboxylates, for example, diethylenetriaminepentaacetic acid (DTPA) Gd-DTPA complexes have been synthesized, which significantly reducing toxicity of the Gd^{3+} ions. In fact, Gd(DTPA) is 50 times less toxic than $GdCl_3$ on a molar basis[20]. It is rapidly cleared with a plasma half-life of 20 minutes, and within 3 hours over 80% is excreted in the urine. On the contrary, only 2% of $GdCl_3$ is excreted after 7 days. $[Gd(DTPA)(H_2O)]^{2-}$ shown in the left panel of Figure 6.1 represents GdDTPA derivatives of Gd chelates based contrast agents. $[Gd(DOTA)(H_2O)]^{-}$ shown in the right panel of Figure 6.1 represents GdDOTA derivatives. Both are thermodynamically stable complexes, very soluble and hydrophilic. However, $[Gd(DOTA)(H_2O)]^{-}$ is very inert to substitution, which makes them very attractive for applications where the contrast agent has a long residency time in the body. $[Gd(DTPA)(H_2O)]^{2-}$ is less inert and can undergo metal ion exchange at low pH[61].

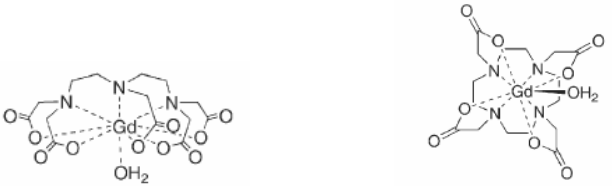

Figure 6.1 Gadolinium complexes $[Gd(DTPA)(H_2O)]^{2-}$ (left) and $[Gd(DOTA)(H_2O)]^{-}$ (right). From Ref.[61].

There is good understanding of the influence of Gd^{3+} ions on relaxation mechanism[73]. In short, the effect originates in dipolar magnetic interaction between the magnetic moment of Gd^{3+} ion and magnetic moments of the protons belonging to water molecules in the vicinity of the ion. Note that the former is due to spin of the electrons while the latter is due to nuclear spin of the proton, so the interaction is quite weak: it decays as $1/R^6$ with increasing distance R between the ion and the proton. Still, molecular motions lead to random fluctuations in this dipolar magnetic interaction, which reduce longitudinal and transverse relaxation times of the protons[62]. The T_1-shortening is, in fact, stronger if concentration of the chelates is low, leading to higher intensity of the signal. Therefore, paramagnetic Gd chelates are mostly used as positive contrast agents. Note that if their concentration increases, the effect may reverse: T_2-shortening effect becomes stronger, the signal intensity decreases, and the contrast could become negative.

The effect of the contrast agent on relaxivity depends on the number of water molecules, their distance to the ion, as well as on the rate of exchange with bulk solvent. Because of the rapid, $1/R^6$ decay of the dipolar magnetic interactions, the reduction of the Gd–H distance would lead to significant increases in relaxivity. However, electron–nuclear double resonance (ENDOR) spectroscopy studies have demonstrated that this distance is about 3.1 Å for a range of Gd ion complexes and does not depend on co-ligand or total charge[74]. Thus, it is unlikely that this distance can be shortened to benefit the relaxivity. Therefore, it is essential that one or more water molecules are present in the inner coordination sphere. Moreover, there should be an exchange of water in and out of the first coordination sphere, which in addition should be fast. At the same time, one should take care of the stability of the complexes with respect to water displacement by endogenous ligands. Different design strategies have been employed[61]. Linear structure of polymer increases the number of Gd ions per molecule but has low relaxivity because of flexibility/internal motion. Dendrimer increases the number of Gd per molecule and introduces more globular structure, slowing rotation and increasing relaxivity, preserving internal motions. Monomer with Gd at barycenter of molecule can be used as well. In this case, although the non-Gd containing arms are free to rotate, the Gd can only rotate at the rate of the entire molecule resulting in high relaxivity. Still,

as complex binding is a reversible process, a small portion of the central ion (Gd^{3+}) may be released from the compound.

At the same time, the gadolinium complexes have certain disadvantages in terms of their clinical applications. In particular, though their excretion through urine is considered as beneficial, the extraction is too rapid leading to short circulating times[75], perhaps too short for high-resolution imaging which still requires long scan times. In addition, relatively weak signal intensity enhancement of such agents makes them less suitable for molecular imaging[76]. Moreover, while some of them were successfully functionalized by bio-targeting groups and/or fluorescent molecules[64], it is not that easy to functionalize them in general with various functional materials, which is a disadvantage for targeting and multimodal imaging. Furthermore, there is a risk of inducing nephrogenic system fibrosis in patients with impaired kidney function, especially in older patients[72].

Summarizing Sec. 6.2 and 6.3, one sees that superparamagnetic Fe-oxide based contrast agents and paramagnetic Gd chelates based contrast agents are commercially available and used as MRI contrast agents. However, the kinetic and thermodynamic stability, the basic pharmacokinetics, side effects and the cost of these agents limit their applications in clinical diagnosis[62]. It is important to solve these problems, and to design new MRI contrast agents, considering different materials systems.

6.4. Gd_2O_3 nanoparticles

One avenue for the design of novel contrast agents is to increase the number of Gd atom that interact with protons. In case of Gd chelates based contrast agents the number of gadolinium atoms interacting with protons is quite high even for smaller samples. However, the potential of crystalline nanoparticles based on inorganic compounds is worth to explore[64]. These systems convey the possibility of high relaxivity. Therefore, using nanoparticles with a ligand that is specific for a certain tissue could enhance the local contrast due to the high relaxivity of each particle. Exploring and optimizing the contrast properties of magnetic nanoparticles based on inorganic compounds, specifically on Gd_2O_3, are therefore important for the design of effective agents with significant contrast enhancement at low concentrations[76].

Gd_2O_3 belongs to the family of so-called sesquioxides. They play very important role in many technological applications, in addition to biomedical applications. In particular, they are used in the processing of ceramics as additives for low-temperature sintering, as grain growth inhibitors, and as phase stabilizers. They are considered in nuclear engineering. They are important optical materials due to their photoluminescence properties[77]. Crystal structure of Gd_2O_3 at room temperature and ambient pressure is most often cubic, though it could also contain admixture, sometimes quite large of the monoclinic phase. With increase of temperature, there is a phase transitions from cubic to monoclinic phase at 1500 K, followed by a transition into hexagonal phase at 2443 K[78]. Three polymorphs of Gd_2O_3 are shown in Figure 6.2. Note that there was a report indicating the different sequence of crystal structure for Gd_2O_3 nanoparticles: they were found to be monoclinic at room temperature, with a transformation into a mixture of the monoclinic and cubic phases between 500 °C and 1000 °C [79].

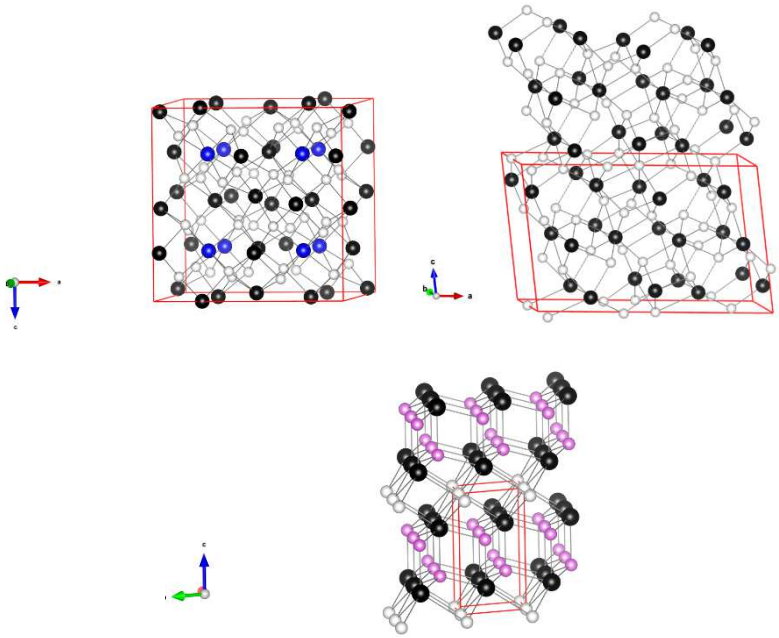

Figure 6.2. Crystal structure of three polymorphs of Gd_2O_3: cubic (top left), monoclinic (top right) and hexagonal (bottom). Gd atoms are shown as dark (black and blue), oxygen atoms are light (white and pink).

Gadolinium oxide has attractive physical properties for technological applications. It has wide optical band gap, 5.2 eV for cubic single-crystal phase of Gd_2O_3, which can be tuned by making it as a thin film in the range 5.0 – 5.4 eV[80]. Of highest interest for this work are remarkable magnetic properties of this material. The electronic configuration of Gd is $(Xe)4f^75d^16s^2$, so the ground state of Gd^{3+} ion has with 7 unpaired electrons with very weak effect of crystal on electronic and magnetic properties of ions (the so-called crystal field splitting is ~0.3 K)[81]. Magnetic interactions between Gd ions in the crystal are expected to be weak leading to paramagnetic behavior over a wide temperature range. Indeed, recent measurements estimated negative value of magnetic ordering temperature from paramagnetic to antiferromagnetic phase – (17.147±0.1)K[82], in agreement with earlier experiment which did not observe any magnetic order in stoichiometric cubic phase of Gd_2O_3 down to 1.2 K[83].

High magnetic properties of bulk Gd_2O_3 motivated substantial interest in exploration of Gd_2O_3 nanoparticles as contrast agents. In 2005 Söderlind *et al.*[27] reported the synthesis and characterization of Gd_2O_3 nanoparticles, prepared by different methods, and the coating of the particles by various carboxylic acids, like oleic and citric acids. Engström *et al.*[76] evaluated the ability of ultra-small (5-10 nm) nanocrystals of gadolinium oxide coated with DEG to perform proton relaxation. Using XPS measurements, Engström *et al.* first verified the oxidation state of the nanoparticles by demonstrating that the peak positions are consistent with the energy level for Gd in bulk Gd_2O_3. Then the authors showed that the relaxivities due to the Gd_2O_3–DEG nanoparticles were twice that of the Gd-DTPA chelate in water solution, almost twice of the chelate relaxivities in buffer, with even more pronounced effect in RPMI. Bridot *et al.*[64] obtained hybrid nanoparticles by encapsulating Gd_2O_3 cores within a polysiloxane shell which carried organic fluorophores and carboxylated PEG covalently tethered to the inorganic network. Their measurements also showed that r_1 of these particles were higher than the positive contrast agents like Gd-DOTA. In addition, the authors demonstrated that their particles can be followed up by fluorescence imaging and proposed that they were suited for dual modality imaging. Moreover, Bridot *et al.* showed that the nanoparticles freely circulate in the blood vessels without undesirable accumulation in lungs and liver. Other crystalline nanoparticles evaluated for applications as contrast agents were based on inorganic or organometallic compounds

of Gd, e.g. gadolinium fluoride nanoparticles, nanorods composed of a metal-organic frameworks built from gadolinium ions and organic bridging ligands (1,4-benzenedicarboxylate)[64].

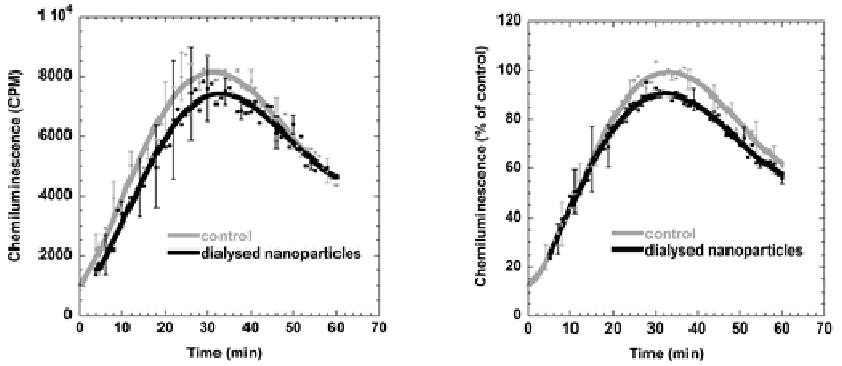

Figure 6.3 Reactive oxygen species (ROS) production measured as luminol-dependent chemiluminescence from neutrophil granulocytes ($2x10^6$/ml) after an initial exposure to dialyzed Gd_2O_3 nanoparticle suspension, followed by a secondary stimulation after 15 minutes with IgG-opsonized yeast particles ($5x10^6$ yeast particles/ml, black traces). Concentration of gadolinium in the suspension is 0.11mM. Left panel represents the mean ± SD of one experiment run in duplicate. Chemiluminescence, given in counts per minute (CPM) was recorded in a Microplate Fluorescence Reader FL600. Right panel shows the mean ± SD of experiments run in duplicate taken from three different donors. The ROS production was calculated as relative chemiluminescence intensity in percentage of control cells treated only with IgG-opsonized yeast particles (shown with gray traces). Republished with permission of IOP Publishing, from Paper I; permission conveyed through Copyright Clearance Center, Inc.

The main synthesis method of Gd_2O_3 nanoparticles in this work was the modified "polyol" route, described in detail in Sec. 2.3. An important point to make here is the need of purification of as-synthesized DEG-Gd_2O_3 nanoparticles suspensions. In most cases the purification step involves dialysis of the nanoparticle samples. Because the synthesis via modified "polyol" route involves dissolution in DEG, the as-synthesized nanoparticles are coated with a layer of diethylene glycol to prevent particle aggregation and there is an excess of ion precursors.

However, the as-synthesized nanoparticles induce too strong inflammatory reaction, as shown in Figure 4.3, and are not suitable for use as the MRI contrast agents. Exchange of DEG to either water or buffer and removal of ions is achieved by the dialysis.

The positive effect of dialysis on biocompatibility of Gd_2O_3 nanoparticles is demonstrated in Figure 6.3, where the neutrophil ROS production is analyzed after an initial exposure to dialyzed Gd_2O_3 nanoparticles, followed by a secondary stimulation after 15 min with IgG-opsonized yeast particles. One can see that the response triggered by the IgG-opsonized yeast particles in the presence of the dialyzed nanoparticles is almost the same as in the control cells, indicating that the ROS production in this case is not significantly altered. For comparison, one sees quite strong inhibition of ROS response upon addition of as synthesized particles, Figure 4.3.

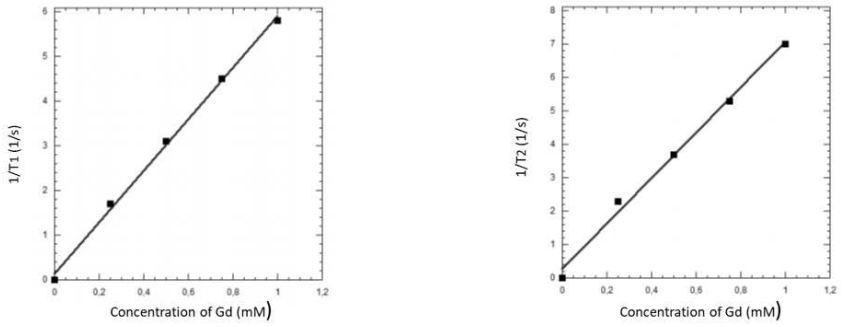

Figure 6.4 Experimentally measured longitudinal relaxation rates $1/T_1$ (left) and transverse relaxation rates $1/T_2$ (right) for dialyzed DEG-Gd_2O_3 nanoparticles.

Experimentally measured longitudinal and transverse relaxation rates for dialyzed DEG-Gd_2O_3 nanoparticles in Milli-Q water are shown in Figure 6.4. Synthesis and dialysis of the nanoparticles, as well as details of measurements are presented in Paper II. Corresponding longitudinal and transverse relaxivities, derived from the data, are as follows: r_1=5.8 $s^{-1}mM^{-1}$ and r_2=6.8 $s^{-1}mM^{-1}$, with r_1/r_2=1.17. The values are higher than the corresponding data for Gd-DTPA, r_1=4.7 $s^{-1}mM^{-1}$ and r_2=5.3 $s^{-1}mM^{-1}$ [76], confirming high potential of Gd_2O_3 nanoparticles for applications as contrast agents.

Chapter 7

Modification of Gd_2O_3 nanoparticles

Though Bazzi *et al*. observed that the modified "polyol" method allowed for a synthesis of the oxide particle suspension, which was colloidally stable for weeks[26] intrinsic instability of the magnetic nanoparticles over longer periods of time is considered as unavoidable problem[19]. Indeed, the small particles tend to form agglomerates to reduce the surface energy. At the same time, one needs a stable injectable solution or a lyophilizate freeze-dried powder that is easy to reconstitute. The challenge is addressed by coating the nanoparticles. The nature of the coating must be optimized to ensure that the coating process is sufficiently simple, the aggregation is effectively prevented, as well as sedimentation of the nanoparticles.

The Gd_2O_3 nanoparticles in this study were synthesized via the modified polyol route[25-26]. In the Gd_2O_3 core synthesis, NaOH is added to induce particles formation of Gd_2O_3 in diethylene glycol (DEG) at a temperature 180^{o}C for at least 4 hours[84]. DEG here acts as both high boiling point solvent and a capping agent via weak interaction on the surface, which can be easily exchanged with other capping agents.

One of the agents that can be chosen for further functionalization of Gd nanoparticles is organosilane. As shown in the Figure 7.1, -OH groups on the top of nanoparticles surface are initial site for the silicon-oxygen-metal bonds through condensation reaction[85]. Furthermore, hydrolysis of silane group generates Si-O-Si polymerized networks, which are much more robust for the stabilization. Therefore, surface silane (see Figure 7.1 (2)) was fabricated by using 3-mercaptopropyl trimethoxy silane (MPTS) with a spacer ligand (see Figure 7.1 (1)) via thiol-maleimide addition reaction. On the other end of the spacer ligand, a reactive NHS ester were kept for further modification. Finally, the surface engineered Gd_2O_3 (see Figure 7.1 (3)) was produced via surface exchanging reaction. Note that the resultant particles, sometimes referred to as PEGylated nanoparticles can be conjugated with commercial dyes for giving high fluorescent properties, Paper II.

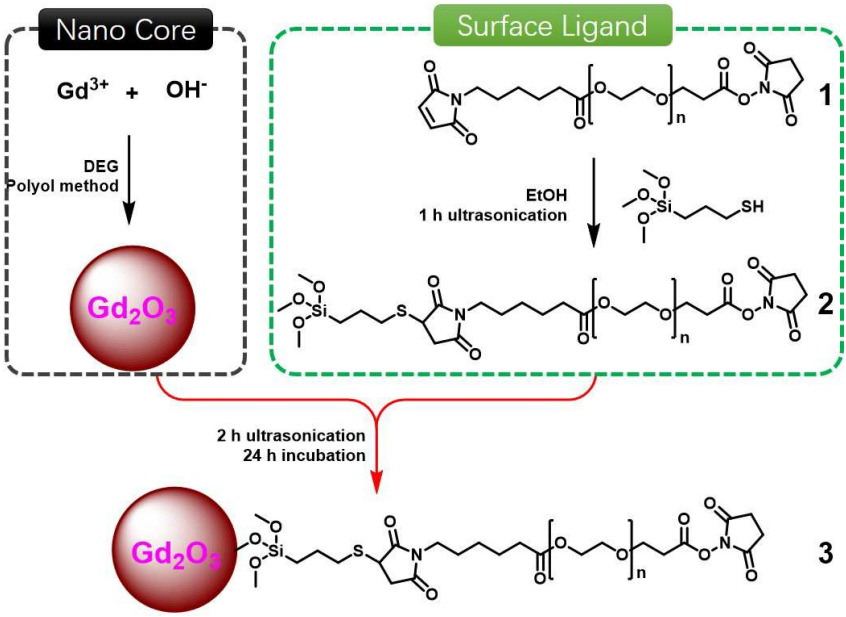

Figure 7.1 Reaction scheme showing the functionalization strategy when capping Gd_2O_3 nanoparticles with (3 Mercaptopropyl) trimethoxysilane (MPTS) and r-Maleinimido-ω carboxysuccinimidyl Ester poly(ethylene glycol) (Mal-PEG-NHS (1)). Nanoparticle solution is added to the Intermediate Molecule (2), and the functionalized nanoparticles (3) are denoted GMP. Adopted from Paper II.

In Paper II it was demonstrated that the dialysis of the nanoparticle samples is of major importance for the use of functionalized Gd NP as MR contrast agent. Indeed, the as-synthesized nanoparticles are coated with a layer of diethylene glycol, which is not appropriate in MRI applications. Dialysis of as-synthesized nanoparticles was discussed in Sec. 6.4. However, free ligands and reaction precursors can also be present in the nanoparticle samples directly after their functionalization, and further dialysis is needed to clear them. The optimization of the dialysis procedure with respect to the choice of membrane, volume, and time has been studied in detail in Paper II. The results for functionalized nanoparticles showed a considerable relaxivity increase for particles dialyzed extensively with r_1 and r_2 values approximately 4 times the corresponding values for Gd-DTPA. Figure 7.2 shows MRI intensity image for PEGylated Gd_2O_3 nanoparticle samples dialyzed for 6 days.

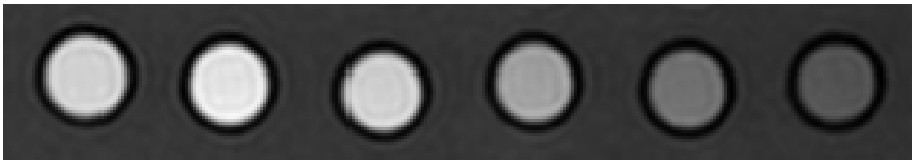

Figure 7.2 T_1-weighed MRI intensity images for PEGylated nanoparticles (GMP) dialyzed for 6 days ordered with decreasing concentration (0.39, 0.19, 0.10, 0.05, 0.02, 0.01mM) from left to right. The images were acquired using a spin echo sequence with TE=20ms and TR=1000ms. Reprinted with permission from Paper II. Copyright 2010 American Chemical Society.

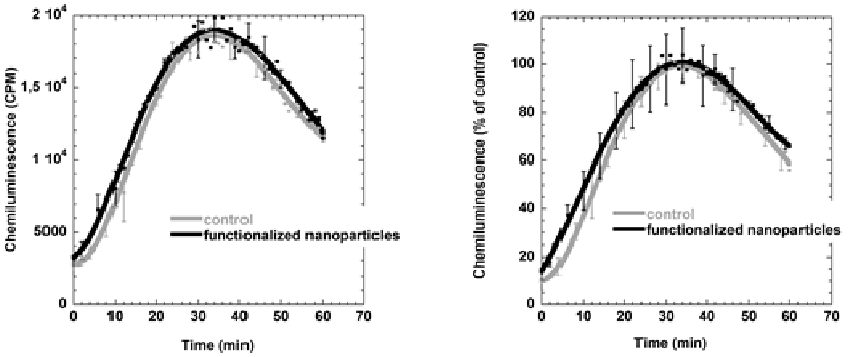

Figure 7.3 Reactive oxygen species (ROS) production measured as luminol-dependent chemiluminescence from neutrophil granulocytes ($2x10^6$ cells/ml) challenged with IgG-opsonized yeast particles ($5x10^6$ yeast particles/ml) after an initial exposure to PEG-functionalized Gd_2O_3 nanoparticles. Concentration of gadolinium in the suspension is 0.02 mM. Left panel represents the mean ± SD of one experiment run in duplicate. Chemiluminescence, given in counts per minute (CPM) was recorded in a Microplate Fluorescence Reader FL600. Right panel shows the mean ± SD of experiments run in duplicate taken from three different donors. The ROS production was calculated as relative chemiluminescence intensity in percentage of control cells treated only with IgG-opsonized yeast particles (shown with gray traces). Republished with permission of IOP Publishing, from Paper I; permission conveyed through Copyright Clearance Center, Inc.

Importantly, surface modification of the Gd nanoparticles with polyethylene glycol improves their biocompatibility, Paper I. Figure 4.3 clearly demonstrates that as-synthesized nanoparticles markedly decreased the ROS production from neutrophils challenged with prey (opsonized yeast particles) compared to controls without nanoparticles. Dialysis of as-synthesized Gd NP leads to more moderate inhibitory effects at a corresponding concentration of gadolinium, as shown in Figure 6.3. Functionalization of the nanoparticles described above further improves their biocompatibility, as demonstrated in Figure 7.3. In fact, the ROS production induced by prey in the presence of a low Gd-concentration of functionalized nanoparticles was similar to the response in cells treated only with IgG-opsonized yeast particles. Moreover, the kinetics of the IgG-opsonized yeast particle induced ROS production in the presence functionalized particles resembles that of the control cells. This was not the case of as-synthesized nanoparticles.

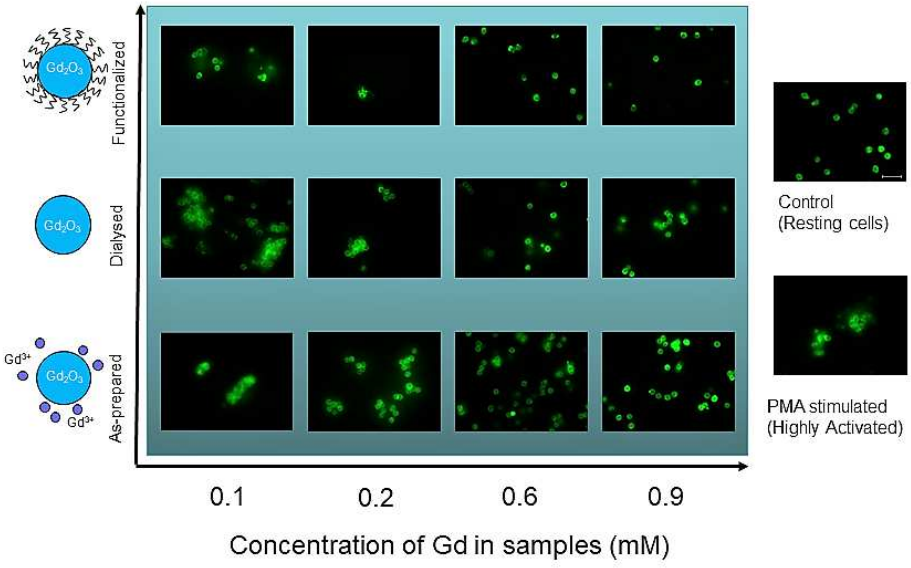

Figure 7.4 Morphological examination of neutrophil granulocytes upon their expose to increasing concentration of as synthesized, dialyzed and functionalized Gd_2O_3 nanoparticles in comparison with the control cells without any exposure and PMA treated (highly activated) cells. The figure shows representative images from 10 images obtained on each treatment. Scale bar indicates 10 µm.). Adopted from Paper I.

Therefore, the PEG-functionalized nanoparticles appear to be better suited for clinical applications.

The conclusion above can be further strengthened by microscopic evaluation of neutrophil morphology discussed in detail in Paper I. Results of a morphological examination with fluorescence microscopy of neutrophil granulocytes upon their expose to increasing concentrations of as synthesized, dialyzed and functionalized Gd_2O_3 nanoparticles are shown in Figure 7.4. Neutrophils were incubated with nanoparticles for 30 minutes at 37°C before fixation in paraformaldehyde, permeabilized and stained for filamentous actin with BODIPY® FL phallacidin. Cells were then visualized in a Zeiss Axioscope with an oil immersion x63/1.4NA objective. Images were captured with a ZVS-47E digital camera together with Easy Image Measurement 2000. In Figure 7.4 one can see increased formation of small, 3–10 neutrophils aggregate and more polarized cells for the as synthesized and dialyzed particles, compared to the untreated control cells with increased Gd concentration. On the contrary, functionalized Gd NP show less pronounced aggregation and their shape appears to be more round at the same concentration of Gd.

Chapter 8

Summary of papers

8.1. Paper I: Effects of gadolinium oxide nanoparticles on the oxidative burst from human neutrophil granulocyte

In Paper I Gd_2O_3 nanoparticles were investigated in a cellular system, as potential probes for visualization and targeting intended for bioimaging applications. The production of reactive oxygen species (ROS) was studied in presence of Gd_2O_3 nanoparticles by means of luminol-dependent chemiluminescence from human neutrophils. The aim of the study was to evaluate a potential nanoparticle induced inflammatory response, as well as their toxic effects on neutrophil granulocytes. As synthesized, dialyzed and PEGylated and dialyzed nanoparticles were investigated.

Gd_2O_3 nanoparticles were synthesized via the modified polyol route[25-26]. A dialysis was performed for 24 h using a 1000 MWCO, Spectra/Por from Spectrum Laboratory Inc. (Breda, The Netherlands) to replace the DEG in the nanoparticle suspension with water, and to remove free ions and potentially small non-mature clusters still left after filtering. For some of the nanoparticle samples surface modification with PEG was carried out, followed by further dialyzes. Neutrophils were isolated from venous whole blood donated by apparently healthy, non-medicated volunteers at Linköping University Hospital, using the method of Böyum[45] presented in Sec. 4.2.

ROS production from neutrophils in suspension upon exposure to as synthesized, dialyzed and PEGylated and dialyzed Gd_2O_3 nanoparticles was studied in 96-well plates using a luminol-dependent chemiluminescence technique[86]. ROS production was detected in a Microplate Fluorescence Reader FL600 (Bio-Tek, Winooski, VT, USA). Results was presented as counts per minute (CPM) or expressed as the relative chemiluminescence intensity as a percentage of that for the control with cells treated only with IgG-opsonized yeast particles (IgG-opsonized yeast particles served as a natural prey for phagocytosis). The data are presented as arithmetical averages ± standard deviation (SD) or standard error of the mean (SEM). When appropriate statistical significance was

evaluated using Student's t-test. The cellular behavior and morphological changes upon expose to all three kinds of nanoparticles were examined by fluorescence staining of the neutrophil actin cytoskeleton.

The obtained results demonstrated that the nanoparticles did not provoke a production of ROS on their own. However, a strong inhibition of neutrophil response to prey was observed after exposure to as synthesized Gd_2O_3 nanoparticles in suspension. We demonstrated that surface modification of the nanoparticles with polyethylene glycol (PEG) is essential in order to increase their biocompatibility. Indeed, the results obtained for dialyzed, and especially for functionalized Gd_2O_3 nanoparticle suspensions showed more moderate inhibitory effects in comparison to neutrophil response to prey observed after exposure to as synthesized Gd_2O_3 nanoparticles at the same concentration of gadolinium. Moreover, at lower gadolinium concentration the response was similar to that of the control cells. The effect of the dialysis was attributed to the removal of the DEG. In fact, we determined the critical concentration of DEG equal to 0.3%, below which the toxic effect was greatly reduced. We therefore concluded that our evaluation of the induced inflammatory response and toxic effects from functionalized nanoparticles makes them promising candidates for the next generation of contrast agents in MRI applications.

8.2. Paper II: Synthesis and Characterization of PEGylated Gd_2O_3 Nanoparticles for MRI Contrast Enhancement

In Paper II, a new design of functionalized ultra-small rare earth-based nanoparticles was reported. The aim of the study was to develop a contrast agent for MRI examination that would be more powerful with respect to both MR signal enhancement and targeting functionality than what was commercially available. Moreover, the nanoparticles were equipped with Rhodamine, allowing for their use as fluorescent probe. We proved that a tag, a fluorescent dye, can be attached to our PEGylated nanoparticles, resulting in the functionalized nanomaterial for targeting purposes.

Small (3-5 nm) Gd_2O_3 nanoparticles were synthesized via the modified polyol route[25-26]. All samples were centrifuge filtered after synthesis to exclude large aggregates, followed by the dialysis. Nanoparticles were functionalized with a bifunctional PEG (Mal-PEG-NHS) via a small silane to investigate, as a proof of concept, possible improvement

of their biocompatibility. In addition, a bifunctional PEG was chosen to enable further tagging to diverse targets. Specifically, PEG functionality was by coupling a fluorophore to the NHS part of the molecule.

The characterization of the nanoparticles and the capping was carried out with various techniques. XPS measurements were performed in a Microlab 310F instrument with a hemispheric analyzer using unmonochromatized Al K_α photons (1486.6 eV). High resolution TEM studies were performed with a FEI Tecnai G2 electron microscope operated at 200 kV. IR spectroscopy studies were carried out on a BrukerVertex 70 FTIR instrument using CaF2 tablets. Dynamic light scattering measurements were performed on an ALV/DLS/SLS-5022F system from ALV-GmbH, Langen, Germany, using a HeNe laser at 632.8 nm with 22 mW output power. Absorbance studies were carried out on an UV-2450 UV-vis spectrophotometer from Shimadzu. Relaxation times were measured with a Philips Achieva 1.5 T whole body MR scanner using the head coil. DLS was primarily used to study the stability of the nanoparticles but also to estimate the hydrodynamic radius of the nanoparticles.

Freshly synthesized nanoparticle samples were stable for weeks at room temperature. Dialyzed samples were more vulnerable, probably since some or most of the DEG capping layer was removed during dialysis. In fact, unfunctionalized dialyzed samples could neither be stored in the freezer nor be treated with NaCl without aggregating to clusters. On the contrary, functionalized samples obtained by using silanes as the innermost stabilizer layer and an outer layer of bifunctional PEG were seen to be stable against both freezing and treatment with NaCl. Most importantly, the functionalized nanoparticle showed substantial increase of relaxation rates compared to unfunctionalized dialyzed samples. Moreover, we found that dialysis carried out to remove free capping agents also improves the relaxivity.

In order to evaluate the Gd_2O_3 nanoparticle induced inflammatory response, we carried out morphological examination of neutrophil granulocytes upon their exposure to as synthesized and functionalized nanoparticles. Peripheral blood used for isolation of neutrophil granulocytes following the method of Böyum [45] and staining of the Actin Cytoskeleton was drawn from apparently healthy, nonmedicated donors at the Linköping University Hospital. Fluorescence microscopy images were acquired using an Axiovert 200 fluorescence microscope with an oil immersion 63x/1.4NA objective (Carl Zeiss GmbH, Germany), and

digital images were obtained using an Axiocam MRm camera and the AxioVision software (version 4.6.3.0). For neutrophils exposed to as syntesized nanoparticles at concentration 0.11mM Gd we observed a clear change in cell morphology compared to negative control cells, indicating their activation. On the contrary, we did not observe extensive activation when neutrophils are exposed to PEGylated Gd_2O_3 nanoparticles, even though concentration was higher, 0.19mM Gd.

8.3. Paper III: Gd_2O_3 nanoparticles in hematopoietic cells for MRI contrast enhancement

In Paper III a study of cell labeling with Gd_2O_3 nanoparticles in hematopoietic cells was presented with the long-term goal to improve techniques for monitoring hematopoietic cells migration with MRI. Starting from an earlier observation that THP-1 monocytes labeled with Gd_2O_3 nanoparticles provide positive contrast in MRI[87]. The aim of this work was to visualize intracellular particles with electron microscopy and to explore whether a hematopoietic progenitor cell line, Ba/F3, would take up the particles or not, and if a transfection agent could further improve uptake in the Ba/F3 cells.

The modified polyol route[25-26] was used for synthesis of the Gd NPs. Because as synthesized nanoparticle samples consisted of different sized particles and contained a large fraction of Gd ions, we performed dialysis to obtain ion-free nanoparticle solutions. The Gd content after 24 hours of dialysis decreased from an initial concentration of 100 mM to about 10 mM.

A hematopoietic progenitor cell line, Ba/F3 and a monocytic cell line, THP-1 were used in this study. The former is a murine pro B-cell line established from mouse fetal liver[88]. The cell line grew in suspension (Roswell Park Memorial Institute 1640 medium with 10% fetal bovine serum, 2 mM L-glutamine, 25 mM HEPES, 50 μM 2-mercaptoethanol, 1% penicillin-streptomycin and 5% interleukin-3 [Sigma-Aldrich, St Louis, MO] and was kept in a cell culture flask at 37°C in 5% carbon dioxide atmosphere. Human monocytic cells THP-1 are phagocytic and grow in suspension (Roswell Park Memorial Institute 1640 medium with 10% fetal bovine serum, 2 mM L-glutamine, 1% penicillin-streptomycin) with the same atmospheric conditions as for Ba/F3. Half of the different cell samples were treated with 10 μg/mL protamine sul-

fate (Sigma-Aldrich Corporation, St Louis, MO). Then cells were incubated with Gd NP in two different concentrations (0.5 mM and 2 mM).

Treated cells were investigated using electron microscopy to visualize intracellular Gd-nanoparticles. An analysis for particle content was carried out by inductively coupled plasma sector field mass spectrometry. MRI was used to assess whether high MRI contrast could be obtained from the Gd_2O_3 nanoparticle-labeled cells. Two experimental sessions were performed to measure relaxation times in the both cell types incubated with Gd NPs with two Gd concentrations specified above, as well as treated and not treated with protamine sulfate, resulting in eight measurements per session. Our study showed that the relaxation times were shortened with increasing particle concentration: longitudinal and transverse relaxivities at 1.5 T and 21°C in different samples were 3.6–5.3 s^{-1} mM^{-1} and 9.6–17.2 s^{-1} mM^{-1}, respectively. Moreover, we demonstrated that protamine sulfate treatment increased the uptake in both Ba/F3 cells and THP-1 cells. Our results demonstrated that Gd_2O_3 nanoparticles were promising as a positive intracellular MRI contrast agent. However, the particles needed to be improved regarding capping stabilizing the particles from degradation as well as from aggregation for further studies on cell labeling,

8.4. Paper IV: Synthesis and characterization of Tb^{3+}-doped Gd_2O_3 nanocrystals: a bifunctional material with combined fluorescent labelling and MRI contrast agent properties

In Paper IV ultra-small gadolinium oxide nanoparticles doped with terbium ions were synthesized as a potentially bifunctional material with both fluorescent and magnetic contrast agent properties. The modified version of the polyol method[25-26] was used for the synthesis, in which 5.7 mM of $GdCl_3 \cdot 6H_2O$ and 0.3 mmol of $TbCl_3 \cdot 6H_2O$ were dissolved in 30 mL of DEG for the 5% Tb-doped Gd_2O_3 nanoparticles (5Tb:Gd), while 1.1 mM of $TbCl_3 \cdot 6H_2O$ was dissolved for 20% Tb-doped Gd_2O_3 nanoparticles (20Tb:Gd). Large sized agglomeration of the particles was removed by filtering of the suspension, followed by an exchange of capping DEG layer using organic acids[27, 84] to obtain the powder form of the product. Functionalization of the nanocrystals with PEG-containing molecules was achieved by grafting the citric acid monohy-

drate (CA-) and dimercaptosuccinic acid (DMSA-) capped particles with HS-PEG-NH_2*HCl and NHSPEG-Mal molecules, respectively.

THP-1 cells were cultured in a cell culture flask in 20-30 mL of RPMI 1640 medium (GIBCO, Invitrogen) with 10% fetal calf serum (FCS), 2 mM L-glutamine, 50 μg/mL streptomycin, and 50 units/mL penicillin. Differentiation of these cells into macrophage like cells was acheived by incubating the cells with 200nM phorbol 12-myristate 13-acetate (PMA) for 72 h. The differentiated cells were loosened from the culture flasks using a cell scraper prior to the experiment. They were incubated for 2 h with 1.0 mM 5%Tb:Gd_2O_3 nanoparticle capped with citric acid, yielding a ratio of 1 million cells/sample. Xenopus laevis dermal fibroblast cells were also investigated in this study.

High-resolution transmission electron microscopy studies were carried out to examine the average size, shape, and crystallinity of the synthesized nanoparticles. The size distribution was similar for the 5% and 20% Tb-doped particles with the average particle size 4.3 nm. The chemical composition of the nanoparticle samples was analyzed with XPS and EDX, which verified the oxidation state and dopant level of the Tb^{3+} ion for the powdered sample. IR spectroscopy was used to verify the presence and properties of the capping molecules. Fluorescence of nanoparticles suspended in water was measured, and the emission spectra of the colloids was found to be typical for Tb^{3+} luminescence. The magnetization behavior of Tb-doped nanoparticles was found to be similar to undoped Gd_2O_3 nanoparticles.

We performed confocal laser scanning microscopy (CLSM) analysis to examine the interaction of the nanoparticles with the cells. Here we used 5Tb:Gd capped with CA. In both cell lines which were treated with the nanoparticles, green fluorescence signals were found. On the contrary, only dim autofluorescence of cells without the addition of the nanoparticles used as the negative controls was found. The luminescent/fluorescent property of the particles were attributable to the Tb^{3+} ion located on the crystal lattice of the Gd_2O_3 host.

MRI relaxivity studies of PEGylated Tb-doped Gd_2O_3 nanoparticles in water media were carried out. The relaxivity values of the both, 5Tb:Gd capped with CA and 5Tb:Gd capped with DMSA were found to be 2-3 times higher than commercially available contrast agent such as Magnevist. Together with the results discussed above showing that gadolinium oxide nanoparticles doped with terbium ions with a size of 4.3 ± 1 nm could be taken up by living cells and that the intracellular con-

centration of these particles allowed fluorescent labeling, the obtained MRI contrast enhancement underlines the bifunctional character of the nanoparticles, which combine luminescent and paramagnetic properties.

8.5. Paper V: Lab-on-a chip for capacitive measurements on human neutrophil granulocytes and their activation triggered by Ce/Gd oxide nanoparticles

In manuscript V neutrophil granulocytes, with rapid cell signaling communicative processes in time frame of minutes, were investigated and their response to cerium-oxide based nanoparticles was monitored using capacitive sensors based on Lab-on-a-chip (LOC) technology. Development of a non-invasive method to monitor cells at work was a long-term goal of the project. The aim of this study was to investigate the possibilities to use the capacitive method to monitor cells with fast response on stimuli and to measure the viability of neutrophils activated at a solid surface. Capacitive measurement is a promising technique to study cells adhering onto a substrate, which was developed recently[9,89-90]. The method is label free and gently measures cells on top of an insulator surface in a weak electric field. On the contrary, in commonly used four-point probes electric measurements the electrodes are in direct contact with cells.

In this work, neutrophils were isolated from venous whole blood donated by healthy, non-medicated volunteers at Linköping University Hospital, a variant of using the method of Böyum[45]. Ce oxide nanoparticles and Ce oxide nanoparticles alloyed with 19% Gd were employed as triggers that induce neutrophils activation. The nanoparticles were prepared using the room temperature wet-chemical synthesis procedure, which was recently were reported in[30]. The nanoparticles were dialyzed and the concentrations of cerium and gadolinium in the prepared nanoparticles were measured with Inductively Coupled Plasma – Mass Spectroscopy by ALS Scandinavia AB.

The complementary metal oxide semiconductor/Low temperature co-fired ceramic (CMOS/LTCC) devices[9, 68] have been employed in this study to monitor the neutrophils activity. Following the uptake of particles neutrophils reduce oxygen to superoxide anions O_2^- through the activation of the enzymatic system, which further metabolize to hydrogen peroxide (H_2O_2) and other even more toxic substances. O_2^-, H_2O_2,

singlet oxygen, and are referred to as reactive oxygen species (ROS)[40]. The cell media surrounding the cells is therefore changing because of the ions released from the cells, and the ionic conductivity starts to dominate change of the sensor output frequency. Ions released to the liquid accumulate on the sensor surface above the electrode and cause capacitance to increase. In addition, when cells are activated they change shape. Therefore, the area of adhesion on the sensor surface may be modified, resulting in a measurable relative capacitive change. The changes of cell morphology and release of charged entities are gently monitored through capacitive measurements utilizing passivation layer on the electrode. This ensures that the cells and (released) compounds are free from direct electrical contacts.

We confirmed that neutrophils settled on the sensor by monitoring frequency change in the sensor signal and additionally by microscopy image. The capacitive response from 16 sensors in parallel was clearly measured and on each sensor just a few cells i.e. about 1-5 cells per sensor were present. Moreover, it was possible to follow the whole process of neutrophil activation stimuli, in form of nanoparticles. This elegantly demonstrated the power of the technique, with the potential to enable single cell measurement.

We therefore concluded that the used in this study delivered high quality results by means of kinetical response, efficiency and sensitivity for fast measurements. Our results demonstrated high potential of such label free method to be used to measure oxidative stress of neutrophil granulocytes, minute by minute.

8.6. Paper VI: Sorbitol capping of gadolinium oxide nanoparticles for magnetic resonance imaging contrast enhancement

In manuscript VI we reported on investigations of interactions of cell with (DEG- Gd_2O_3) nanoparticles both capped to and immersed in Sorbitol, including measurements of the reactive oxygen species production by neutrophils using the effect of chemiluminescence. High magnetic properties of crystalline Gd_2O_3 motivated substantial interest in exploration of Gd_2O_3 nanoparticles (GdNP) as contrast agents. This motivated intense research to ensure safe and efficient biomedical applications of this type of nanoparticles. In this work we exploit a promising path provided by surface modification of the nanoparticles. We studied if the capping of GdNP with the Sorbitol improves their biocompatibility.

The Gd_2O_3 nanoparticles were synthesized via the modified "polyol" route[25-26]. In the Gd_2O_3 core synthesis, we followed the protocol presented in[84], adding the Sorbitol in concentration 6 mmol in the last half hour. To exclude aggregates and ions, the particle solution was filtered and dialyzed in Milli-Q water. In addition, dialyzed GdNP without Sorbitol coating were synthesized. Part of the dialyzed GdNP were immersed in Sorbitol. Comparison of the results for the three sets of the nanoparticles, dialyzed GdNP, dialyzed GdNP caped with Sorbitol, and dialyzed GdNP immersed in Sorbitol allows for a direct evaluation of the effect of the Sorbitol coating. The hydrodynamic radius of sorbitol coated GdNP as obtained from the Dynamic Light Scattering (DLS) experiment was estimated to be 2.04 ±0.3 nm.

The performance of different nanoparticles synthesized in this work as MRI contrast agents was evaluated by measurements of their relaxivity. The measurements were done for all three kinds of nanoparticles solutions, as well as for the mouse alveolar cell line MH-S incubated with dialyzed GdNP. Bruker minispec mq60 NMR analyzer was employed in this work. Relaxation studies showed that results obtained for GdNP capped to Sorbitol were essentially the same as for dialyzed GdNP, indicating that the surface modification does not directly affects the relaxivity. On the other hand, significantly different relaxation times for samples of macrophages incubated with different nanoparticles synthesized in this work were measured, indicating the increased uptake of GdNP capped to Sorbitol by the cells, and that the Sorbitol is indeed captured by the nanoparticles rather than released into solution during the synthesis. This can explain contrast enhancement of 228% was observed for the cells incubated with Sorbitol caped GdNP, reported in[91].

Further, we have considered the interactions of the studied nanoparticles with neutrophil granulocytes. ROS production from neutrophils exposed to dialyzed Gd oxide NP and dialyzed Sorbitol capped nanoparticles was traced for 1 h. The dialyzed Sorbitol capped NP sample have displayed significant ROS scavenging properties compared to the control and improved biocompatibility in comparison with dialyzed Gd oxide NP.

Finally, neutrophils morphology was evaluated as a parameter of the nanoparticle induced inflammatory response by means of the fluorescence microscopy. Isolated neutrophils were counted in a bürkner chamber, and the cell concentration was adjusted to 2 x 10^6 cells/mL.

The cells were kept on ice until exposed to dialyzed GdNP and nanoparticles caped with Sorbitol or for 30 min under stirring condition at 37ºC. Samples were then fixed in 4% paraformaldehyde for 30 min, washed three times in PBS, permeabilized and stained for F-actin by incubation with 100 μg/mL lysophosphatidylcholine and 0.6 μg/mL bodipy-phallacidin in PBS for 30 min at room temperature in darkness[92]. After triplicate washing, the cells were visualized in a Nikon Eclipse TI-TIRF/ Epi-fl Illuminator Unit. Images were captured with a Nikon DS-Fi2 digital camera. the fluorescence microscopy has confirmed that the capping of the nanoparticles in Sorbitol enhances the cell compatibility for neutrophils.

Taking together the remarkable contrast enhancement observed for the cells incubated with Sorbitol caped GdNP[91] and their improved biocompatibility, we conclude that Sorbitol capping of gadolinium oxide nanoparticles is promising for the design of next generation of MRI contrast agents.

Chapter 9

Conclusions and outlook

In my project the potential of using several types of nanoparticles as tools in various biomedical applications was investigated. Nanoscience gives lot of hope to improving quality of live. In my case, the use of new contrast agents for the clinically important diagnostic technique, magnetic resonance imaging (MRI) should lead to more efficient and accurate diagnostic of various diseases, and eventually save lives. However, nanoparticles may be harmful to patients, and therefore they have to be well tested to insure their safety. A traditional, but out-of-its-time approach would require large number of animal tests, for instance on mice. In this work we developed and used modern approaches that allowed for investigations of cell-nanoparticle interactions.

It is important to point out that addressing the challenge of a development of next generation of biocompatible MRI contrast agents calls for consistent international efforts. For example, in 2007, the US Science Council presented a new toxicity test strategy in the "Toxicity Testing in the 21st Century: A Vision and a Strategy" report. The document proposed a whole new strategy for risk assessment of chemicals by replacing animal tests with more predictive tests. The goal is more efficient, cheaper and more relevant risk assessment of chemicals and combinations of chemicals. This will happen with increased knowledge of the effects on humans and with the help of new cell tests.

In Sweden, the development of methods for replacement, reduction and refinement of animal experiments is recognized as highly important task. The goal of this project was to investigate biocompatibility of promising Gd_2O_3 nanoparticles synthesized in our group. These nanoparticles are selected on the basis of their physical properties, that is they show enhanced magnetic properties and therefore may be of high potential interest for applications as contrast agents.

Such studies require close collaboration between disciplines i.e. medicine, biology, chemistry and physics and one striking advantage of this approach is that the outcome of several nanoparticle functionalization strategies may be evaluated by means of physical characterization, probing capability and biological activity already at an early stage, during design and optimization of a new type of nanoparticle.

It is of great importance that administration of nanoparticles *in vivo*, e.g. to an individual during an MRI examination, does not inhibit important cell functions or cause extensive cell activation, possibly leading to an impaired response upon infection. To study the cell nanoparticle interactions, I used several cell types, including isolated blood cells neutrophil granulocytes. Neutrophils are white blood cells participating in our defense against invading microbes. *In vitro* studies carried out in this work included investigation of the effects of Gd_2O_3 nanoparticles on the function of neutrophil granulocytes. Their biocompatibility was improved with various techniques, e.g. functionalization with PEG and capping with Sorbitol.

REFERENCES

1. Bhattacharya, K.; Farcal, L.; Fadeel, B., Shifting identities of metal oxide nanoparticles: Focus on inflammation. *MRS Bulletin* **2014,** *39* (11), 970-975.
2. Chelikowsky, J. R., Nanostructures, Electronic Structure of. In *Encyclopedia of Condensed Matter Physics*, Bassani, F.; Liedl, G. L.; Wyder, P., Eds. Elsevier: Oxford, 2005; pp 51-58.
3. Bansmann, J.; Baker, S. H.; Binns, C.; Blackman, J. A.; Bucher, J. P.; Dorantes-Dávila, J.; Dupuis, V.; Favre, L.; Kechrakos, D.; Kleibert, A.; Meiwes-Broer, K. H.; Pastor, G. M.; Perez, A.; Toulemonde, O.; Trohidou, K. N.; Tuaillon, J.; Xie, Y., Magnetic and structural properties of isolated and assembled clusters. *Surface Science Reports* **2005,** *56* (6), 189-275.
4. Tal, A. A.; Olovsson, W.; Abrikosov, I. A., Origin of the core-level binding energy shifts in Au nanoclusters. *Physical Review B* **2017,** *95* (24), 245402.
5. Hjerrild, N. E.; Taylor, R. A., Boosting solar energy conversion with nanofluids. *Physics Today* **2017,** *70* (12), 40-45.
6. Hagemeyer, A.; Volpe, A., Catalysts: Materials. In *Encyclopedia of Condensed Matter Physics*, Bassani, F.; Liedl, G. L.; Wyder, P., Eds. Elsevier: Oxford, 2005; pp 158-165.
7. Posada-Borbón, A.; Heard, C. J.; Grönbeck, H., Cluster Size Effects in Ethylene Hydrogenation over Palladium. *The Journal of Physical Chemistry C* **2017,** *121* (20), 10870-10875.
8. Shtepliuk, I.; Caffrey, N. M.; Iakimov, T.; Khranovskyy, V.; Abrikosov, I. A.; Yakimova, R., On the interaction of toxic Heavy Metals (Cd, Hg, Pb) with graphene quantum dots and infinite graphene. *Scientific Reports* **2017,** *7* (1), 3934.
9. Halonen, N.; Kilpijarvi, J.; Sobocinski, M.; Datta-Chaudhuri, T.; Hassinen, A.; Prakash, S. B.; Moller, P.; Abshire, P.; Kellokumpu, S.; Lloyd Spetz, A., Low temperature co-fired ceramic packaging of CMOS capacitive sensor chip towards cell viability monitoring. *Beilstein J Nanotechnol* **2016,** *7*, 1871-1877.
10. Hu, Z.; Ahrén, M.; Selegård, L.; Skoglund, C.; Söderlind, F.; Engström, M.; Zhang, X.; Uvdal, K., Highly Water-Dispersible Surface-Modified Gd2O3 Nanoparticles for Potential Dual-Modal Bioimaging. *Chemistry – A European Journal* **2013,** *19* (38), 12658-12667.
11. Wang, G.; Zhang, X.; Liu, Y.; Hu, Z.; Mei, X.; Uvdal, K., Magneto-fluorescent nanoparticles with high-intensity NIR emission, T1-

and T2-weighted MR for multimodal specific tumor imaging. *Journal of Materials Chemistry B* **2015,** *3* (15), 3072-3080.
12. Coey, J. M. D.; Ni Mhiocháin, T. R., Magnetism, History of. In *Encyclopedia of Condensed Matter Physics*, Bassani, F.; Liedl, G. L.; Wyder, P., Eds. Elsevier: Oxford, 2005; pp 227-236.
13. Wang, G.; Zhang, X.; Skallberg, A.; Liu, Y.; Hu, Z.; Mei, X.; Uvdal, K., One-step synthesis of water-dispersible ultra-small Fe3O4 nanoparticles as contrast agents for T1 and T2 magnetic resonance imaging. *Nanoscale* **2014,** *6* (5), 2953-2963.
14. Subhankar, B.; Wolfgang, K., Supermagnetism. *Journal of Physics D: Applied Physics* **2009,** *42* (1), 013001.
15. Ahrén, M.; Selegård, L.; Söderlind, F.; Linares, M.; Kauczor, J.; Norman, P.; Käll, P.-O.; Uvdal, K., A simple polyol-free synthesis route to Gd2O3 nanoparticles for MRI applications: an experimental and theoretical study. *Journal of Nanoparticle Research* **2012,** *14* (8), 1006.
16. Reddy, L. H.; Arias, J. L.; Nicolas, J.; Couvreur, P., Magnetic Nanoparticles: Design and Characterization, Toxicity and Biocompatibility, Pharmaceutical and Biomedical Applications. *Chemical Reviews* **2012,** *112* (11), 5818-5878.
17. Hergt, R.; Dutz, S.; Müller, R.; Zeisberger, M., Magnetic particle hyperthermia: nanoparticle magnetism and materials development for cancer therapy. *Journal of Physics: Condensed Matter* **2006,** *18* (38), 2919-2934.
18. Jordan, A.; Wust, P.; Fähling, H.; John, W.; Hinz, A.; Felix, R., Inductive heating of ferrimagnetic particles and magnetic fluids: Physical evaluation of their potential for hyperthermia. *International Journal of Hyperthermia* **2009,** *25* (7), 499-511.
19. Laurent, S.; Forge, D.; Port, M.; Roch, A.; Robic, C.; Vander Elst, L.; Muller, R. N., Magnetic Iron Oxide Nanoparticles: Synthesis, Stabilization, Vectorization, Physicochemical Characterizations, and Biological Applications. *Chemical Reviews* **2008,** *108* (6), 2064-2110.
20. Fricker, S. P., The therapeutic application of lanthanides. *Chemical Society Reviews* **2006,** *35* (6), 524-533.
21. Robbins, E. J.; Leckenby, R. E.; Willis, P., The ionization potentials of clustered sodium atoms. *Advances in Physics* **1967,** *16* (64), 739-744.
22. Knight, W. D.; Clemenger, K.; de Heer, W. A.; Saunders, W. A.; Chou, M. Y.; Cohen, M. L., Electronic Shell Structure and Abundances of Sodium Clusters. *Physical Review Letters* **1984,** *52* (24), 2141-2143.

23. de Heer, W. A., The physics of simple metal clusters: experimental aspects and simple models. *Reviews of Modern Physics* **1993,** *65* (3), 611-676.
24. Pilch, I.; Söderström, D.; Brenning, N.; Helmersson, U., Size-controlled growth of nanoparticles in a highly ionized pulsed plasma. *Applied Physics Letters* **2013,** *102* (3), 033108.
25. Bazzi, R.; Flores-Gonzalez, M. A.; Louis, C.; Lebbou, K.; Dujardin, C.; Brenier, A.; Zhang, W.; Tillement, O.; Bernstein, E.; Perriat, P., Synthesis and luminescent properties of sub-5-nm lanthanide oxides nanoparticles. *Journal of Luminescence* **2003,** *102-103* (4), 445-450.
26. Bazzi, R.; Flores, M. A.; Louis, C.; Lebbou, K.; Zhang, W.; Dujardin, C.; Roux, S.; Mercier, B.; Ledoux, G.; Bernstein, E.; Perriat, P.; Tillement, O., Synthesis and properties of europium-based phosphors on the nanometer scale: Eu2O3, Gd2O3:Eu, and Y2O3:Eu. *Journal of Colloid and Interface Science* **2004,** *273* (1), 191-197.
27. Söderlind, F.; Pedersen, H.; Petoral, R. M.; Käll, P.-O.; Uvdal, K., Synthesis and characterisation of Gd2O3 nanocrystals functionalised by organic acids. *Journal of Colloid and Interface Science* **2005,** *288* (1), 140-148.
28. Ahrén, M.; Selegård, L.; Klasson, A.; Söderlind, F.; Abrikossova, N.; Skoglund, C.; Bengtsson, T.; Engström, M.; Käll, P.-O.; Uvdal, K., Synthesis and Characterization of PEGylated Gd2O3 Nanoparticles for MRI Contrast Enhancement. *Langmuir* **2010,** *26* (8), 5753-5762.
29. SelegÅrd, L.; Khranovskyy, V.; Söderlind, F.; Vahlberg, C.; Ahrén, M.; Käll, P.-O.; Yakimova, R.; Uvdal, K., Biotinylation of ZnO Nanoparticles and Thin Films: A Two-Step Surface Functionalization Study. *ACS Applied Materials & Interfaces* **2010,** *2* (7), 2128-2135.
30. Eriksson, P.; Tal, A. A.; Skallberg, A.; Brommesson, C.; Hu, Z.; Boyd, R. D.; Olovsson, W.; Fairley, N.; Abrikosov, I. A.; Zhang, X.; Uvdal, K., Cerium oxide nanoparticles with antioxidant capabilities and gadolinium integration for MRI contrast enhancement. *Scientific Reports* **2018,** *8* (1), 6999.
31. Meshkian, R.; Dahlqvist, M.; Lu, J.; Wickman, B.; Halim, J.; Thörnberg, J.; Tao, Q.; Li, S.; Intikhab, S.; Snyder, J.; Barsoum, M. W.; Yildizhan, M.; Palisaitis, J.; Hultman, L.; Persson, P. O. Å.; Rosen, J., W-Based Atomic Laminates and Their 2D Derivative W1.33C MXene with Vacancy Ordering. *Advanced Materials* **2018,** *30* (21), 1706409.

32. Inouye, K.; Endo, R.; Otsuka, Y.; Miyashiro, K.; Kaneko, K.; Ishikawa, T., Oxygenation of ferrous ions in reversed micelle and reversed microemulsion. *The Journal of Physical Chemistry* **1982,** *86* (8), 1465-1469.
33. De Jaeger, N.; Demeyere, H.; Finsy, R.; Sneyers, R.; Vanderdeelen, J.; van der Meeren, P.; van Laethem, M., Particle Sizing by Photon Correlation Spectroscopy Part I: Monodisperse latices: Influence of scattering angle and concentration of dispersed material. *Particle & Particle Systems Characterization* **1991,** *8* (1-4), 179-186.
34. Pennycook, S. J., Transmission Electron Microscopy. In *Encyclopedia of Condensed Matter Physics*, Bassani, F.; Liedl, G. L.; Wyder, P., Eds. Elsevier: Oxford, 2005; pp 240-247.
35. Jiang, Y.; Chen, Z.; Han, Y.; Deb, P.; Gao, H.; Xie, S.; Purohit, P.; Tate, M. W.; Park, J.; Gruner, S. M.; Elser, V.; Muller, D. A., Electron ptychography of 2D materials to deep sub-ångström resolution. *Nature* **2018,** *559* (7714), 343-349.
36. Berne, B. J.; Pecora, R., Dynamic light scattering: with applications to chemistry, biology, and physics. 2000. *Mineola, NY: Dover Publications* **2000,** *376*.
37. Ferrando, R.; Jellinek, J.; Johnston, R. L., Nanoalloys: From Theory to Applications of Alloy Clusters and Nanoparticles. *Chemical Reviews* **2008,** *108* (3), 845-910.
38. Murphy, K. P.; Murphy, K. M.; Travers, P.; Walport, M.; Janeway, C.; Mauri, C.; Ehrenstein, M., *Janeway's Immunobiology*. Garland Science: 2008.
39. Scher, J. U.; Abramson, S. B.; Pillinger, M. H., Neutrophils I. In *Fundamentals of Inflammation*, Serhan, C. N.; Gilroy, D. W.; Ward, P. A., Eds. Cambridge University Press: Cambridge, 2010; pp 39-48.
40. Cassatella, M. A., Neutrophils II. In *Fundamentals of Inflammation*, Serhan, C. N.; Gilroy, D. W.; Ward, P. A., Eds. Cambridge University Press: Cambridge, 2010; pp 49-64.
41. Boraschi, D.; Italiani, P.; Palomba, R.; Decuzzi, P.; Duschl, A.; Fadeel, B.; Moghimi, S. M., Nanoparticles and innate immunity: new perspectives on host defence. *Seminars in Immunology* **2017,** *34*, 33-51.
42. Goncalves, D. M.; de Liz, R.; Girard, D., Activation of Neutrophils by Nanoparticles. *TheScientificWorldJOURNAL* **2011,** *11*, 9.
43. Sanfins, E.; Correia, A.; B. Gunnarsson, S.; Vilanova, M.; Cedervall, T., Nanoparticle effect on neutrophil produced myeloperoxidase. *PLOS ONE* **2018,** *13* (1), e0191445.

44. Malech, H. L., The Role of Neutrophils in the Immune System. In *Neutrophil Methods and Protocols*, Quinn, M. T.; DeLeo, F. R.; Bokoch, G. M., Eds. Humana Press: Totowa, NJ, 2007; Vol. 412, pp 3-11.
45. Böyum, A., Isolation of mononuclear cells and granulocytes from human blood. Isolation of monuclear cells by one centrifugation, and of granulocytes by combining centrifugation and sedimentation at 1 g. *Scandinavian journal of clinical and laboratory investigation. Supplementum* **1968,** *97*, 77-89.
46. Kolaczkowska, E.; Kubes, P., Neutrophil recruitment and function in health and inflammation. *Nature Reviews Immunology* **2013,** *13*, 159.
47. Hocking, W. G.; Golde, D. W., The Pulmonary-Alveolar Macrophage. *New England Journal of Medicine* **1979,** *301* (11), 580-587.
48. Mbawuike, I. N.; Herscowitz, H. B., MH-S, a Murine Alveolar Macrophage Cell Line: Morphological, Cytochemical, and Functional Characteristics. *Journal of Leukocyte Biology* **1989,** *46* (2), 119-127.
49. Auwerx, J., The human leukemia cell line, THP-1: A multifacetted model for the study of monocyte-macrophage differentiation. *Experientia* **1991,** *47* (1), 22-31.
50. Daley, G. Q.; Baltimore, D., Transformation of an interleukin 3-dependent hematopoietic cell line by the chronic myelogenous leukemia-specific P210bcr/abl protein. *Proceedings of the National Academy of Sciences* **1988,** *85* (23), 9312-9316.
51. Rabi, I. I.; Zacharias, J. R.; Millman, S.; Kusch, P., A New Method of Measuring Nuclear Magnetic Moment. *Physical Review* **1938,** *53* (4), 318-318.
52. Purcell, E. M.; Torrey, H. C.; Pound, R. V., Resonance Absorption by Nuclear Magnetic Moments in a Solid. *Physical Review* **1946,** *69* (1-2), 37-38.
53. Bloch, F.; Hansen, W. W.; Packard, M., The Nuclear Induction Experiment. *Physical Review* **1946,** *70* (7-8), 474-485.
54. Bloch, F.; Hansen, W. W.; Packard, M., Nuclear Induction. *Physical Review* **1946,** *69* (3-4), 127-127.
55. Wehrli, F. W., The origins and future of nuclear magnetic resonance imaging. *Physics Today* **1992,** *45* (6), 34-42.
56. Pankhurst, Q. A.; Connolly, J.; Jones, S. K.; Dobson, J., Applications of magnetic nanoparticles in biomedicine. *Journal of Physics D: Applied Physics* **2003,** *36* (13), R167.

57. Lauterbur, P. C., Image Formation by Induced Local Interactions: Examples Employing Nuclear Magnetic Resonance. *Nature* **1973,** *242*, 190.
58. Lauterbur, P. C., All Science Is Interdisciplinary—From Magnetic Moments to Molecules to Men (Nobel Lecture). *Angewandte Chemie International Edition* **2005,** *44* (7), 1004-1011.
59. Mansfield, P., Multi-planar image formation using NMR spin echoes. *Journal of Physics C: Solid State Physics* **1977,** *10* (3), L55.
60. Paul C. Lauterbur, P. M., The Nobel Prize in Physiology or Medicine 2003 - Speed Read. Nobel Media AB: 2014.
61. Caravan, P., Strategies for increasing the sensitivity of gadolinium based MRI contrast agents. *Chemical Society Reviews* **2006,** *35* (6), 512-523.
62. Yan, G.-P.; Robinson, L.; Hogg, P., Magnetic resonance imaging contrast agents: Overview and perspectives. *Radiography* **2007,** *13*, e5-e19.
63. Capelletti, R., Luminescence. In *Encyclopedia of Condensed Matter Physics*, Bassani, F.; Liedl, G. L.; Wyder, P., Eds. Elsevier: Oxford, 2005; pp 178-189.
64. Bridot, J.-L.; Faure, A.-C.; Laurent, S.; Rivière, C.; Billotey, C.; Hiba, B.; Janier, M.; Josserand, V.; Coll, J.-L.; Vander Elst, L.; Muller, R.; Roux, S.; Perriat, P.; Tillement, O., Hybrid Gadolinium Oxide Nanoparticles: Multimodal Contrast Agents for in Vivo Imaging. *Journal of the American Chemical Society* **2007,** *129* (16), 5076-5084.
65. Patching, S. G., Surface plasmon resonance spectroscopy for characterisation of membrane protein–ligand interactions and its potential for drug discovery. *Biochimica et Biophysica Acta (BBA) - Biomembranes* **2014,** *1838* (1, Part A), 43-55.
66. Hawk, R. M.; Armani, A. M., Label free detection of 5′ hydroxymethylcytosine within CpG islands using optical sensors. *Biosensors and Bioelectronics* **2015,** *65*, 198-203.
67. Xu, Y.; Xie, X.; Duan, Y.; Wang, L.; Cheng, Z.; Cheng, J., A review of impedance measurements of whole cells. *Biosensors and Bioelectronics* **2016,** *77*, 824-836.
68. Datta-Chaudhuri, T.; Abshire, P.; Smela, E., Packaging commercial CMOS chips for lab on a chip integration. *Lab on a Chip* **2014,** *14* (10), 1753-1766.
69. Enochs, W. S.; Harsh, G.; Hochberg, F.; Weissleder, R., Improved delineation of human brain tumors on MR images using a long-circulating, superparamagnetic iron oxide agent. *Journal of Magnetic Resonance Imaging* **1999,** *9* (2), 228-232.

70. Semelka, R. C.; Helmberger, T. K. G., Contrast Agents for MR Imaging of the Liver. *Radiology* **2001,** *218* (1), 27-38.
71. Weissleder, R.; Elizondo, G.; Wittenberg, J.; Rabito, C. A.; Bengele, H. H.; Josephson, L., Ultrasmall superparamagnetic iron oxide: characterization of a new class of contrast agents for MR imaging. *Radiology* **1990,** *175* (2), 489-493.
72. Hu, F.; Zhao, Y. S., Inorganic nanoparticle-based T1 and T1/T2 magnetic resonance contrast probes. *Nanoscale* **2012,** *4* (20), 6235-6243.
73. Lowe, M. P., MRI Contrast Agents: The Next Generation. *Australian Journal of Chemistry* **2002,** *55* (9), 551-556.
74. Astashkin, A. V.; Raitsimring, A. M.; Caravan, P., Pulsed ENDOR Study of Water Coordination to Gd3+ Complexes in Orientationally Disordered Systems. *The Journal of Physical Chemistry A* **2004,** *108* (11), 1990-2001.
75. Kim, B. H.; Lee, N.; Kim, H.; An, K.; Park, Y. I.; Choi, Y.; Shin, K.; Lee, Y.; Kwon, S. G.; Na, H. B.; Park, J.-G.; Ahn, T.-Y.; Kim, Y.-W.; Moon, W. K.; Choi, S. H.; Hyeon, T., Large-Scale Synthesis of Uniform and Extremely Small-Sized Iron Oxide Nanoparticles for High-Resolution T1 Magnetic Resonance Imaging Contrast Agents. *Journal of the American Chemical Society* **2011,** *133* (32), 12624-12631.
76. Engström, M.; Klasson, A.; Pedersen, H.; Vahlberg, C.; Käll, P.-O.; Uvdal, K., High proton relaxivity for gadolinium oxide nanoparticles. *Magnetic Resonance Materials in Physics, Biology and Medicine* **2006,** *19* (4), 180-186.
77. Zhang, F. X.; Lang, M.; Wang, J. W.; Becker, U.; Ewing, R. C., Structural phase transitions of cubic Gd2O3 at high pressures. *Physical Review B* **2008,** *78* (6), 064114.
78. Zinkevich, M., Thermodynamics of rare earth sesquioxides. *Progress in Materials Science* **2007,** *52* (4), 597-647.
79. Jamnezhad, H.; Jafari, M., Structure of Gd2O3 nanoparticles at high temperature. *Journal of Magnetism and Magnetic Materials* **2016,** *408*, 164-167.
80. Singh, M. P.; Thakur, C. S.; Shalini, K.; Banerjee, S.; Bhat, N.; Shivashankar, S. A., Structural, optical, and electrical characterization of gadolinium oxide films deposited by low-pressure metalorganic chemical vapor deposition. *Journal of Applied Physics* **2004,** *96* (10), 5631-5637.
81. Moon, R. M.; Koehler, W. C., Magnetic properties of Gd2O3. *Physical Review B* **1975,** *11* (4), 1609-1622.
82. Mele, P.; Artini, C.; Ubaldini, A.; Costa, G. A.; Carnasciali, M. M.; Masini, R., Synthesis, structure and magnetic properties in the

Nd2O3–Gd2O3 mixed system synthesized at 1200°C. *Journal of Physics and Chemistry of Solids* **2009,** *70* (2), 276-280.
83. Miller, A. E.; Jelinek, F. J.; Jr., K. A. G.; Gerstein, B. C., Low-Temperature Magnetic Behavior of Several Oxides of Gadolinium. *The Journal of Chemical Physics* **1971,** *55* (6), 2647-2648.
84. Pedersen, H.; Söderlind, F.; Petoral, R. M.; Uvdal, K.; Käll, P.-O.; Ojamäe, L., Surface interactions between Y2O3 nanocrystals and organic molecules—an experimental and quantum-chemical study. *Surface Science* **2005,** *592* (1), 124-140.
85. Neouze, M.-A.; Schubert, U., Surface Modification and Functionalization of Metal and Metal Oxide Nanoparticles by Organic Ligands. *Monatshefte für Chemie - Chemical Monthly* **2008,** *139* (3), 183-195.
86. Dahlgren, C.; Karlsson, A., Respiratory burst in human neutrophils. *Journal of Immunological Methods* **1999,** *232* (1), 3-14.
87. Klasson, A.; Ahrén, M.; Hellqvist, E.; Söderlind, F.; Rosén, A.; Käll, P.-O.; Uvdal, K.; Engström, M., Positive MRI Enhancement in THP-1 Cells with Gd2O3 Nanoparticles. *Contrast Media and Molecular Imaging* **2008,** *3* (3), 106-111.
88. Palacios, R.; Henson, G.; Steinmetz, M.; McKearn, J. P., Interleukin-3 supports growth of mouse pre-B-cell clones in vitro. *Nature* **1984,** *309*, 126.
89. Prakash, S. B.; Abshire, P., Tracking cancer cell proliferation on a CMOS capacitance sensor chip. *Biosensors and Bioelectronics* **2008,** *23* (10), 1449-1457.
90. Senevirathna, B. P.; Lu, S.; Dandin, M. P.; Basile, J.; Smela, E.; Abshire, P. A., Real-Time Measurements of Cell Proliferation Using a Lab-on-CMOS Capacitance Sensor Array. *IEEE Transactions on Biomedical Circuits and Systems* **2018,** *12* (3), 510-520.
91. Larsson, E. Evaluation of the Dual-Modal usage of contrast agents by means of Synchrotron X-ray Computed Microtomography and Magnetic Resonance Imaging using Macrophages loaded with Barium Sulfate and Gadolinium Nanoparticles for Detection and Monitoring in Animal Disease Models. P.hD. Thesis, LiU-Tryck, Linköping, 2015.
92. Bengtsson, T.; Zalavary, S.; Stendahl, O.; Grenegard, M., Release of oxygen metabolites from chemoattractant-stimulated neutrophils is inhibited by resting platelets: role of extracellular adenosine and actin polymerization. *Blood* **1996,** *87* (10), 4411-4423.

Papers

The papers associated with this thesis have been removed for copyright reasons. For more details about these see:

http://urn.kb.se/resolve?urn=urn:nbn:se:liu:diva-152347